

High Density QCD and Instantons

R. Rapp¹, T. Schäfer², E. V. Shuryak¹ and M. Velkovsky³

¹ *Department of Physics and Astronomy, State University of New York, Stony Brook, NY 11794-3800*

² *School of Natural Sciences, Institute for Advanced Study, Princeton, NJ 08540*

³ *Nuclear Theory Group, Brookhaven National Laboratory, Upton, NY 11973-5000*

(April 19, 2022)

Instantons generate strong non-perturbative interactions between quarks. In the vacuum, these interactions lead to chiral symmetry breaking and generate constituent quark masses on the order of 300-400 MeV. The observation that the same forces also provide attraction in the scalar diquark channel leads to the prediction that cold quark matter is a color superconductor, with gaps as large as ~ 100 MeV. We provide a systematic treatment of color superconductivity in the instanton model. We show that the structure of the superconductor depends on the number of flavors. In the case of two flavors, we verify the standard scenario and provide an improved calculation of the mass gap. For three flavors, we show that the ground state is color-flavor locked and calculate the chiral condensate in the high density phase. We show that as a function of the strange quark mass, there is a sharp transition between the two phases. Finally, we go beyond the mean-field approximation and investigate the role of instanton-antiinstanton molecules, which – besides superconducting gap formation – provide a competitive mechanism for chiral restoration at finite density.

I. INTRODUCTION

Studying Quantum Chromodynamics (QCD) at finite baryon density does not require a special motivation: this is, after all, the traditional subject of nuclear physics. Nevertheless, the investigation of cold quark matter lay dormant for some time and was only revived recently when it was realized that a number of exciting new phenomena can be predicted with some certainty. The first is that we expect the high density phase of QCD to be a color superconductor, with sizeable gaps on the order of 100 MeV around the phase transition [1,2]. The structure of this phase depends sensitively on the number of active flavors. For three or more flavors, color and flavor quantum numbers are locked and chiral symmetry is broken even at large chemical potential μ [3,4]. In addition to that, it was argued that the second order chiral phase transition at finite temperature T and zero density is likely to turn first order at some critical density. This entails the existence of a tricritical point in the $\mu - T$ phase diagram, which would persist even if the light quarks are not massless [5–7].

The idea that asymptotic freedom and the presence of a sharp Fermi surface imply that high density QCD should be a color superconductor goes back to the work of Frautschi, Barrois, Bailin and Love [8–10]. Color superconductivity has many features of the standard model, such as dynamical gauge symmetry breaking and the Higgs phenomenon. It is different from electroweak symmetry breaking in the standard model in the sense that the Higgs is composite. And it is different from models with compositeness (such as technicolor) in that it does not require strong interactions. Color superconductivity takes place even in weak coupling. This, of course, is a consequence of the BCS instability.

Detailed numerical calculations of color superconducting gaps were carried out by Bailin and Love, who concluded that one-gluon exchange (OGE) induces gaps on the order of 1 MeV at several times nuclear matter density (at asymptotically large chemical potentials, however, magnetic gluon exchanges generate increasingly large gaps [11]). The main new feature pointed out in [1,2] is that instanton-induced interactions can lead to substantially larger gaps, on the order of 100 MeV. Furthermore, it was realized that the phase structure of QCD at finite baryon density is very rich. Besides the dominant order parameter for the superconducting phase transition, which is a scalar-isoscalar color antitriplet diquark operator, many other forms are possible.

Previous work mostly concentrated on two or three massless flavors and was based on the mean-field approximation (MFA). In the present work, we go beyond these approximations in several important respects. In the case of two flavors we replace schematic zero range interactions with the full momentum dependent instanton-induced interaction [12–14]. We study the three-flavor case and show that the ground state exhibits color-flavor locking. We show that chiral symmetry is broken, calculate the chiral condensate, and also assess the effects of a finite strange quark mass. In order to go beyond the mean field approximation we study the role of instanton-antiinstanton clusters. In particular, we consider the competition between random instantons and clusters employing a statistical mechanics treatment of the partition function for the instanton liquid. Finally, we consider more speculative possibilities such as phases with diquark Bose condensation, and give a general discussion of the phase structure of QCD with different quark masses.

Throughout the article we assume that instanton-induced effects are the predominant source of strong non-perturbative interactions in cold quark matter at small and moderate densities. This assumption is based on the

success of the instanton model at zero temperature and zero chemical potential, as well as at $\mu = 0$ and $T \neq 0$, see [15] for a review. The other major type of interaction that has been widely used is the (perturbative) OGE. While the latter should be prevailing at high densities, it encounters conceptual difficulties at low and moderate densities since the involved momentum transfers at the Fermi surface $q^2 \leq p_F^2$, and the running coupling constant of QCD might not be sufficiently small as required for a perturbative treatment. On the other hand, the Debye-screening of electric fields suppresses instanton effects at large densities; however, this suppression seems not to be effective below the chiral phase transition, as has been explicitly demonstrated in finite- T lattice studies [16,17].

Further evidence for the importance of instantons in this context is related to the existence of fermion zero modes in the spectrum of the Dirac operator, which arise as a consequence of the axial anomaly: In a topologically non-trivial background field with topological charge $+1$ there is – for each flavor – a left-handed state that emerges out of the Dirac sea, and a right-handed one that moves from positive to negative energy. As a result, the axial charge is violated by $2N_f$ units. For $N_f = 1$ this immediately implies chiral condensation. For more than one flavor, chiral condensation is a collective effect. The quark condensate is determined by the number density of (almost) zero modes of the Dirac operator. These anomalously small eigenmodes can originate from the interaction of exact zero modes associated with isolated instantons and antiinstantons. The wave function of the condensate is the collective state built from instanton and antiinstanton zero modes. To check this mechanism for chiral symmetry breaking on the lattice has lately attracted appreciable attention: the results indeed support the suggested picture [18,19].

At finite baryon chemical potential the axial anomaly is connected with fermion zero modes in exactly the same way as in vacuum. The only difference is that the zero modes now correspond to extra states appearing at the Fermi surface, rather than the surface of the Dirac sea. As in the vacuum the effect of the zero modes can be represented as an effective $(2N_f)$ -quark interaction that operates near the Fermi surface. For two flavors, this interaction directly leads to the BCS instability, the formation of Cooper pairs and the appearance of a gap. For three and more flavors the instanton vertex does not directly support a Cooper pair; some of the chiral condensates have to be non-zero to close off external quark legs, reducing the N_f -body instanton interaction to a two-body one. Instanton-antiinstanton molecules, on the other hand, lead to an effective four quark operator for any number of flavors, which, if attractive, will trigger the formation of a gap. Nevertheless, direct instantons play an important role even for $N_f \geq 3$. In particular, instantons provide a novel mechanism for chiral condensation: A diquark-driven $\bar{q}q$ (chiral) condensate.

The investigation of chiral symmetry restoration and color superconductivity at finite density should also be placed in a broader context, *e.g.*, including finite temperatures. Moreover, we would like to understand the phase structure as a function of parameters that we cannot control in the real world, such as the number of flavors and their masses. After all, the underlying mechanisms for the various transitions and the role of non-perturbative effects (such as instantons) in the different phases have to be clarified.

At high temperature we expect to find a quark-gluon plasma phase in which chiral symmetry is restored, *i.e.*, the density of (almost) zero modes has to vanish. This can be realized if the instanton liquid changes from a random ensemble of instantons and antiinstantons to a correlated system with finite clusters, *e.g.*, instanton-antiinstanton (I - A) molecules. The formation of molecules and other correlated clusters was observed in numerical simulations of the instanton liquid [20], where a number of consequences of this scenario were explored. On the lattice the disappearance of the quasi-zero modes in the vicinity of T_c is well established, and the formation of clusters has been observed [21]. Nevertheless, many details of the transition remain to be understood. In the case of many flavors the instanton calculations [22] suggest a chirally restored vacuum state already for a fairly small number of flavors, around 5. Again, the transition is associated with the formation of correlated clusters.

In this article we would like to understand the interplay of the three major phases that have been considered: (i) the hadronic (H) phase, with (strongly) broken chiral symmetry (ii) the color superconductor (CSC) phase, with broken color symmetry, and (iii) the quark-gluon plasma (QGP) phase. All three phases are associated with three specific instanton-induced interactions. Chiral symmetry breaking is caused by the strong $\bar{q}q$ attraction. The binding energy of the lightest baryon, the nucleon, is mostly associated with the qq interaction. The same interaction is responsible for superconductivity at large baryon density. Finally, quark exchanges between instantons and antiinstantons drive their pairing, which is expected to become the predominant feature in the instanton liquid as temperature increases (at any chemical potential).

The structure of our paper is as follows. The first part, comprised of sects. II-VII contains a mean-field analysis of color superconductivity in finite-density QCD with 2 and 3 flavors. We begin with a brief introduction to the structure of the effective instanton-induced interaction in sect. II. In sect. III, we study the physical effects of this interaction in different diquark channels at $\mu = 0$. In sect. IV we discuss the modifications of the instanton-induced interactions at non-zero chemical potential. The interplay of chiral symmetry breaking and quark superconductivity in two-flavor QCD is studied in sect. V. This section employs the mean-field approximation but is based on the exact form of the interaction. Using a simplified version of the form factors we then consider different $\langle \bar{q}q \rangle$ and $\langle qq \rangle$ condensates of increasing complexity: the three-flavor problem in the chiral limit (sect. VI) and the effect of flavor symmetry breaking due to a finite strange quark mass (sect. VII).

The second part of the article (sect. VIII and IX) addresses effects due to clustering, which are beyond the mean-field approximation. In sect. VIII we quantitatively discuss only one type of cluster, the instanton-antiinstanton molecule, which we believe is the most important cluster in the chirally restored phase. In sect. IX, we also discuss the role of correlations between quarks – in particular non-condensed diquarks and (the most obvious cluster of all!) nucleons in nuclear matter –, and comment on possible experimental consequences for heavy-ion reactions and neutron stars. We summarize and conclude in sect. X.

II. EFFECTIVE INSTANTON-INDUCED INTERACTIONS IN VACUUM

A. Single-Instanton Interactions

Our starting point is the euclidean QCD partition function

$$\mathcal{Z} = \int \mathcal{D}\psi \mathcal{D}\psi^\dagger \mathcal{D}A \exp(-S_{QCD}) = \int \mathcal{D}A \det(\mathcal{D}) \exp(-S_{gauge}) . \quad (1)$$

The main assumption of the instanton model is that the gauge field is saturated by classical (anti-)instanton solutions. If the instanton ensemble is sufficiently dilute, the gauge field can be approximated by a sum of individual instanton gauge potentials

$$A = \sum_{k \in I, \bar{I}} A_k . \quad (2)$$

Collective effects related to chiral symmetry breaking are generated through the low-momentum part of the fermion determinant. In particular, we will concentrate on the fermion determinant in a basis spanned by the zero modes of the individual instantons. Matrix elements of the Dirac operator in this basis are given by the overlap integrals

$$T_{IA}(z, u) = \int d^4x \phi_I^\dagger(x - z_I) \mathcal{D} \phi_A(x - z_A) . \quad (3)$$

Here, z_I and z_A denote the positions of the instanton and antiinstanton, and $\phi_{I,A}$ the corresponding zero mode wave functions, which are solutions of the Dirac equation

$$\mathcal{D}_{I,A} \phi_{I,A}(x) = 0 , \quad (4)$$

where the covariant derivative $\mathcal{D}_{I,A}$ includes the gauge potential of the (anti-) instanton I (A). Using the Dirac equation (4) and the sum ansatz (2), Eq. (3) can be simplified by replacing the covariant derivative by an ordinary one. The overlap matrix element can also be viewed as the quark “hopping” amplitude from an instanton to an antiinstanton.

To extract effective $2N_f$ -quark interaction vertices, we follow the approach of Diakonov and Petrov [23], who suggested to reintroduce free fermion fields according to

$$\mathcal{Z} = \int d\psi d\psi^\dagger \frac{\exp\{\int d^4x \psi^\dagger i \mathcal{D} \psi\}}{N_+! N_-!} \prod_{I=1}^{N_+} \theta_+ \prod_{\bar{I}=1}^{N_-} \theta_- , \quad (5)$$

where in the two-flavor case

$$\theta_+ = \int d\Omega_I \prod_{f=1}^2 \left[\int d^4x \psi_f^\dagger(x) i \mathcal{D} \phi_I(x - z_I) \int d^4y \phi_I^\dagger(y - z_I) i \mathcal{D} \psi_f(y) \right] , \quad (6)$$

and the integrals are over the collective coordinates $\Omega_I = \{z_I, \rho_I, u_I\}$ (position, size and color orientation) of the instantons. The original zero mode determinant can be recovered by calculating a Green’s function with $N_f(N_+ + N_-)$ external legs. In order to perform the integration over the centers of the instantons it is convenient to proceed to momentum space. This automatically induces a four-momentum conserving δ -functions at each vertex.

An effective interaction is most easily derived by exponentiating the fermion terms. This is accomplished by applying an inverse Laplace transformation which gives the following partition function:

$$\mathcal{Z} = \text{const} \int d\psi d\psi^\dagger d\beta_+ d\beta_- \exp \left\{ -(N_+ + 1) \log \left(\frac{\beta_+}{c_\rho} \right) - (N_- + 1) \log \left(\frac{\beta_-}{c_\rho} \right) \right. \\ \left. + \int d^4x (\psi^\dagger i \not{\partial} \psi + \beta_+ \theta_+ + \beta_- \theta_-) \right\}. \quad (7)$$

The integrations over β_\pm can be performed by the saddle point method, which becomes exact in the thermodynamic limit as the coefficients in the exponent are extensive quantities ($N_\pm = n_\pm V_4$). For an equal number of instantons and antiinstantons, one may consider $g = \beta_+ = \beta_-$ as an effective fermion coupling. β_\pm are then eliminated through the final minimization of the free energy, leaving the total instanton density $N/V = n_+ + n_-$ as the physical parameter.

In the remainder of this section we restrict ourselves to two flavors. In this case, four quarks participate at each vertex, and the pertinent vertex operator θ_\pm takes the form

$$\mathcal{O}_{\theta_+} = \prod_{f=1}^2 d\Omega_f (\Omega_f \chi_L) \otimes (\chi_R^\dagger \Omega_f^\dagger). \quad (8)$$

Its non-locality can be expressed through a momentum-dependent formfactor $\mathcal{F}(k)$, which is also a matrix in the Dirac space, attached to each fermion field. We will analyze the formfactors, including their dependence on density, in sect. IV B. After color-averaging, one obtains the effective interaction lagrangian

$$\mathcal{L} = g \frac{1}{4(N_c^2 - 1)} \left\{ \frac{2N_c - 1}{2N_c} [(\bar{\psi} \mathcal{F}^\dagger \tau_\alpha^- \mathcal{F} \psi)^2 + (\bar{\psi} \mathcal{F}^\dagger \gamma_5 \tau_\alpha^- \mathcal{F} \psi)^2] \right. \\ \left. + \frac{1}{4N_c} (\bar{\psi} \mathcal{F}^\dagger \sigma_{\mu\nu} \tau_\alpha^- \mathcal{F} \psi)^2 \right\}, \quad (9)$$

where N_c is the number of colors and $\tau^- = (\vec{\tau}, i)$ is an isospin matrix. In the pseudoscalar channel the interaction combines attraction for the isospin-1 (pion) channel with repulsion (due to the extra i) for isospin-0 (η'). Similarly, one finds attraction in the scalar isospin-0 (σ) channel (responsible for spontaneous chiral symmetry breaking) together with repulsion in the scalar isospin-1 channel (a_0).

In practice we will calculate correlation functions and the mean field effective potential in the Hartree-Fock approximation. For this purpose, it is convenient to construct an effective s -channel kernel including the exchange term. This is made possible by the simple (separable) form of the momentum dependence. Using this kernel, one can reproduce the result of a Hartree-Fock calculation by evaluating the Hartree term only. In short-hand notation we will refer to the kernel as the effective meson or diquark lagrangian. From the Fierz identities given in appendix A, we obtain the following kernel for color singlet and octet $\bar{q}q$ states

$$\mathcal{L}_{mes} = \frac{g}{8N_c^2} \left\{ [(\bar{\psi} \mathcal{F}^\dagger \tau^- \mathcal{F} \psi)^2 + (\bar{\psi} \mathcal{F}^\dagger \tau^- \gamma_5 \mathcal{F} \psi)^2] \right. \\ \left. + \frac{N_c - 2}{2(N_c^2 - 1)} [(\bar{\psi} \mathcal{F}^\dagger \tau^- \lambda^a \mathcal{F} \psi)^2 + (\bar{\psi} \mathcal{F}^\dagger \tau^- \lambda^a \gamma_5 \mathcal{F} \psi)^2] \right. \\ \left. - \frac{N_c}{4(N_c^2 - 1)} (\bar{\psi} \mathcal{F}^\dagger \tau^- \sigma_{\mu\nu} \lambda^a \mathcal{F} \psi)^2 \right\}, \quad (10)$$

again being attractive in the σ and π channel, repulsive in the η' and a_0 channel. Analogously, we can construct the effective interaction for color-antisymmetric $\bar{\mathbf{3}}$ and -symmetric $\mathbf{6}$ diquarks. The result is

$$\mathcal{L}_{diq} = \frac{g}{8N_c^2} \left\{ -\frac{1}{N_c - 1} [(\psi^T \mathcal{F}^T C \tau_2 \lambda_A^a \mathcal{F} \psi)(\bar{\psi} \mathcal{F}^\dagger \tau_2 \lambda_A^a C \mathcal{F}^* \bar{\psi}^T \right. \\ \left. + (\psi^T \mathcal{F}^T C \tau_2 \lambda_A^a \gamma_5 \mathcal{F} \psi)(\bar{\psi} \mathcal{F}^\dagger \tau_2 \lambda_A^a \gamma_5 C \mathcal{F}^* \bar{\psi}^T)] \right. \\ \left. + \frac{1}{2(N_c + 1)} (\psi^T \mathcal{F}^T C \tau_2 \lambda_S^a \sigma_{\mu\nu} \mathcal{F} \psi)(\bar{\psi} \mathcal{F}^\dagger \tau_2 \lambda_S^a \sigma_{\mu\nu} C \mathcal{F}^* \bar{\psi}^T) \right\}, \quad (11)$$

where τ_2 is the antisymmetric Pauli matrix, and $\lambda_{A,S}$ are the antisymmetric (color $\bar{\mathbf{3}}$) and symmetric (color $\mathbf{6}$) color generators (normalized in an unconventional way, $\text{tr}(\lambda^a \lambda^b) = N_c \delta^{ab}$, in order to facilitate the comparison between mesons and diquarks). In the color $\bar{\mathbf{3}}$ channel, the interaction is attractive for scalar ($\psi^T C \gamma_5 \psi$) diquarks, and repulsive for pseudoscalar ($\psi^T C \psi$) diquarks.

As we have already discussed in our previous paper [2], in the case of two-color ($N_c=2$) QCD there exists an additional Pauli-Gürsey symmetry (PGSY) [24,25] which mixes quarks with antiquarks. It also manifests itself in the

lagrangians given above, as in this case the coupling constants in $\bar{q}q$ and qq channels are identical, *i.e.*, diquarks (the baryons of the $N_c=2$ -theory) are degenerate with the corresponding mesons. Chiral symmetry breaking then implies that scalar diquarks are also Goldstone bosons, with their mass vanishing in the chiral limit (*i.e.*, for current quark masses $m = 0$).

B. I - A -Molecule Induced Interactions

Using the 't Hooft interaction introduced in the last section one can calculate correlation functions in a systematic expansion in multi-instanton interactions, starting from direct instantons graphs and proceeding to two-instanton or instanton-antiinstanton graphs, as well as more complicated clusters. In simple cases, like the set of RPA diagrams discussed in sect. III, one can sum a whole series of terms involving infinitely many instantons. But if the instanton ensemble is strongly correlated, this method may become very inefficient. In that case it is more useful to determine the effective vertex for a given cluster, and fix the strength of the vertex by calculating the concentration of clusters from the partition function. The simplest kind of cluster that can arise in the instanton ensemble are instanton-antiinstanton molecules. We have observed the formation of these clusters at high temperature and at large N_f in both analytic [26,27] and numerical simulations of the instanton ensemble [20]. In these cases, molecules are intimately connected with chiral symmetry restoration. An ensemble of molecules does not have delocalized zero modes or collective eigenstates, and the chiral condensate is zero.

In the high density problem, the role of molecules is twofold. First, the concentration of instanton-antiinstanton molecules in the ensemble may be dynamically enhanced for similar reasons as in the case of high temperature or large number of flavors. We will discuss this problem in detail in sect. VIII. Second, the BCS instability is due to quark-quark scattering, or four-fermion operators. The 't Hooft vertex is a $(2N_f)$ -fermion operator and does not automatically lead to an instability for $N_f > 2$. However, an instanton-antiinstanton molecule can always generate an effective four-fermion interaction, with the additional $(2N_f - 4)$ fermion lines being internal.

The effective four-fermion vertex induced by instanton-antiinstanton molecules was evaluated in [28]. The result is particularly simple if the relative color orientation is fixed such that the instanton-antiinstanton interaction is most attractive. In that case one has

$$\mathcal{L}_{IA} = G_{mol} \left\{ \frac{1}{N_c^2} [(\bar{\psi}\gamma_\mu\psi)^2 + (\bar{\psi}\gamma_\mu\gamma_5\psi)^2] - \frac{1}{2N_c(N_c-1)} [(\bar{\psi}\gamma_\mu\lambda^a\psi)^2 + (\bar{\psi}\gamma_\mu\gamma_5\lambda^a\psi)^2] \right. \\ \left. - \frac{1}{N_c^2} [(\bar{\psi}\gamma_\mu\psi)^2 - (\bar{\psi}\gamma_\mu\gamma_5\psi)^2] - \frac{2N_c-1}{2N_c(N_c-1)} [(\bar{\psi}\gamma_\mu\lambda^a\psi)^2 - (\bar{\psi}\gamma_\mu\gamma_5\lambda^a\psi)^2] \right\}. \quad (12)$$

Similar to the procedure leading to Eq. (11), this interaction can be rearranged into an effective qq vertex. In the color antitriplet channel the result is

$$\mathcal{L}_{IA}^3 = G_{mol} \left\{ \frac{1}{N_c(N_c-1)} [(\psi^T C \gamma_5 \tau_2 \lambda_A^a \psi)(\bar{\psi} \gamma_5 \tau_2 \lambda_A^a C \bar{\psi}^T) - (\psi^T C \tau_2 \lambda_A^a \psi)(\bar{\psi} \tau_2 \lambda_A^a C \bar{\psi}^T)] \right. \\ \left. + \frac{1}{4N_c(N_c-1)} [(\psi^T C \gamma_\mu \gamma_5 \tau_2 \lambda_A^a \psi)(\bar{\psi} \gamma_\mu \gamma_5 \tau_2 \lambda_A^a C \bar{\psi}^T) - (\psi^T C \gamma_\mu \tau_2 \lambda_A^a \psi)(\bar{\psi} \gamma_\mu \tau_2 \lambda_A^a C \bar{\psi}^T)] \right\}. \quad (13)$$

Even in the case $N_f = 2$, there are two important differences as compared to the single-instanton vertex. First, since molecules are topologically neutral, the interaction is $U(1)_A$ invariant. This implies that it does not distinguish between scalar and pseudoscalar diquarks. Second, whereas the 't Hooft vertex only operates in scalar (and tensor) channels, molecules also provide an interaction in vector-meson and diquark channels. The coupling constant is related to the density of molecules and has to be determined from the partition function of the instanton liquid. We will study this problem in sect. VIII E.

III. DIQUARKS IN THE RANDOM PHASE APPROXIMATION

Color superconductivity implies that the high density phase is composed of diquark Cooper pairs. In a weakly coupled BCS system, the expression 'Cooper pair' should not be taken too literally: it is not tightly bound and the range of its wave function is large compared to average inter-particle separations (*i.e.*, the cube root of the inverse particle density, $d = n^{-3/2}$). In QCD this is not necessarily the case. The gap can be quite large, and the existence of an intermediate phase of diquarks with or without Bose condensation is not a priori excluded.

For this reason we first study the possibility of diquark bound states in vacuum [29,30,25]. In QCD with $N_c > 2$ there are, of course, no gauge invariant diquark states. Instead, one can study correlation functions of heavy-light Qqq states, where the heavy quark Q serves to neutralize color. Effectively, this corresponds to a diquark correlator in the presence of a Wilson line. The “gauge invariant” diquark masses extracted from these correlators then measure the mass of the heavy Qqq state minus the mass of the heavy quark. In a dense medium, the Wilson line is not necessary, and color is neutralized by light quarks of the third color.

In the effective fermionic theory derived in the previous section, diquarks can appear as physical bound states. These states should be interpreted as building blocks in the formation of baryons and dense matter. In practice, we study diquark correlation functions and look for poles in the diquark propagators at momenta $|p| < 2M$, where M is the constituent quark mass. For simplicity, instead of the exact instanton formfactors $\mathcal{F}(p)$, we employ in this section an euclidean $O(4)$ symmetric cutoff Λ , being adjusted to yield a realistic constituent quark mass M .

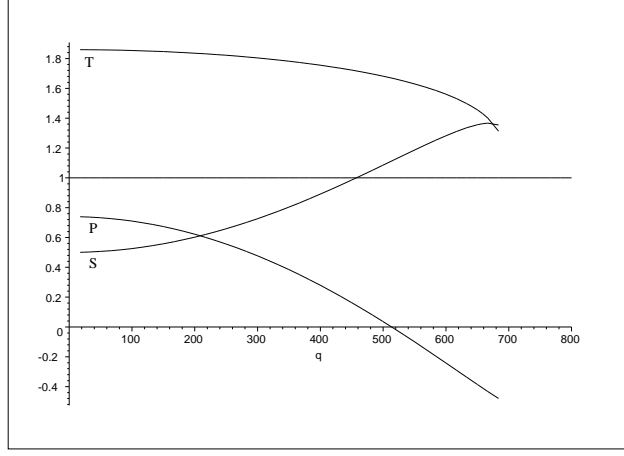


FIG. 1. The quantity KJ entering the denominators of the T matrix for the scalar (S), pseudoscalar (P) and tensor (T) diquark channels.

The Bethe-Salpeter equation for the two-body \mathcal{T} matrix in a given channel can be written as

$$\mathcal{T}(q) = \sum_i K_i (C^{-1} \mathcal{O}^i) \times \left\{ (\mathcal{O}^i C) + i \text{tr} \int \frac{d^4 p}{(2\pi)^4} S_F(p + q/2) (\mathcal{O}^i C) S_F^T(-p + q/2) \mathcal{T}(q) \right\}. \quad (14)$$

Introducing the notation

$$\mathcal{T}(q) = \sum_{k,k'} (C^{-1} \mathcal{O}^k) T_{k,k'}(q) (\mathcal{O}^{k'} C), \quad (15)$$

Eq. (14) can be expressed schematically as

$$T = K(1 + JT). \quad (16)$$

This equation has the solution

$$T = (1 - KJ)^{-1} K. \quad (17)$$

In both diquark and mesonic channels J takes the form

$$J_{k,k'}(p) = i \text{tr} \int \frac{d^4 p}{(2\pi)^4} S_F(p + q/2) \mathcal{O}^k S_F(p - q/2) \mathcal{O}^{k'}, \quad (18)$$

since $C S_F^T(p) C^{-1} = S_F(-p)$. From Eq. (11) one has the three different operator structures, $\mathcal{O} = \tau_2 \lambda_A^a i \gamma_5$ (scalar channel), $\mathcal{O} = \tau_2 \lambda_A^a$ (pseudoscalar channel) and $\mathcal{O} = \tau_2 \lambda_S^a \sigma_{\mu\nu}$ (tensor channel), which lead to

$$\begin{aligned} J_{SS} &= -2I_1(M) + 2q^2 I_2(q^2, M) \\ J_{PP} &= 2I_1(M) + 2(4M^2 - q^2) I_2(q^2, M) \\ J_{TT} &= -16M^2 I_2(q^2, M) \end{aligned} \quad (19)$$

with the two standard integrals

$$I_1(M) = 8N_c \int_0^\Lambda \frac{d^4p}{(2\pi)^4} \frac{1}{p^2 + M^2} \quad (20)$$

$$I_2(-q^2, M) = 4N_c \int_0^\Lambda \frac{d^4p}{(2\pi)^4} \frac{1}{(p + 1/2q)^2 + M^2} \frac{1}{(p - 1/2q)^2 + M^2} . \quad (21)$$

They are readily evaluated for Euclidean momenta and analytically continued to Minkowski space to yield

$$I_1(M) = \frac{N_c}{2\pi^2} \left[\Lambda^2 + M^2 \ln \frac{M^2}{\Lambda^2 + M^2} \right], \quad (22)$$

$$I_2(q^2, M) = \frac{N_c}{4\pi^2} \left[\ln \frac{M^2}{\Lambda^2 + M^2} + 2\sqrt{\frac{4M^2 - q^2}{q^2}} \arctan \sqrt{\frac{q^2}{4M^2 - q^2}} \right. \\ \left. - 2 \left(1 - \frac{2\Lambda^2}{4(\Lambda^2 + M^2) - q^2} \right) \sqrt{\frac{4(\Lambda^2 + M^2) - q^2}{q^2}} \arctan \sqrt{\frac{q^2}{4(\Lambda^2 + M^2) - q^2}} \right]. \quad (23)$$

The chiral gap equation in the scalar $\bar{q}q$ channel then becomes

$$\frac{g}{8N_c^2} I_1(M) = 1, \quad (24)$$

which provides a relation between the coupling g and the constituent quark mass M .

The conditions for the existence of poles in the corresponding channels of the diquark \mathcal{T} matrix are

$$- \frac{g}{8N_c^2(N_c - 1)} (-2I_1(M) + 2q^2 I_2(q^2, M)) = 1 \quad (25)$$

for the scalar channel,

$$- \frac{g}{8N_c^2(N_c - 1)} (2I_1(M) + 2(4M^2 - q^2) I_2(q^2, M)) = 1, \quad (26)$$

for the pseudoscalar one and

$$\frac{g}{16N_c(N_c + 1)} (-16M^2 I_2(q^2, M)) = 1 \quad (27)$$

for the tensor one. If the *l.h.s.* crosses 1, there is a bound state. This is illustrated in Fig. 1 where we have taken $M = 350$ MeV, $\Lambda = 900$ MeV for definiteness. One finds that only the scalar diquark is bound, with a binding energy of about 200 MeV.

This result agrees with numerical simulations of the instanton liquid [30], which included all diagrams in this interaction. However, it is at variance with the conclusion drawn in [25], where no bound scalar diquark was found in the same model. We believe that the discrepancy is due to the fact that the authors of [25] only used part of the interaction in the diquark channel. In this work, we have performed a Hartree-Fock calculation with the full one-instanton interaction. A lattice calculation of diquark masses was performed in [31]. These authors find a significant scalar-vector diquark mass splitting, but no scalar diquark bound state. On the other hand, they also obtained a too small N - Δ mass splitting, and a mass ratio m_N/m_ρ that is too large.

One can also argue that there should be some continuity when going from the theory with $N_c = 2$ to $N_c = 3$. In the former case the scalar diquark is the partner of the pion and the vector diquark is the partner of ρ . This implies that the scalar diquark binding is large, $M_{dq,V} - m_{dq,S} = m_\rho - m_\pi \simeq 600$ MeV. It is then natural that some remnant of the binding is left at $N_c = 3$, since the coupling constant in the scalar diquark channel for $N_c = 3$ is only reduced by a factor of 2 as compared to the $N_c = 2$ case. This corresponds to a “ $N_c = 2 + \epsilon$ ” picture of the baryon octet: a tightly bound scalar diquark loosely coupled to the third quark. A number of phenomenological observations (reviewed, *e.g.*, in [32]) actually supports the validity of this picture for real QCD. The decuplet baryons, on the other hand, do not contain scalar diquarks, and therefore should be generic 3-body objects. This picture is quite contrary to another (and much better known) view of baryonic structure, the large N_c limit. Here both N , Δ as well as other members of the octet and decuplet are basically the same heavy object, slowly rotating with slightly different angular momenta. Indeed, as one reads off from the lagrangians given in the previous section, in this limit the diquark coupling tends to zero, and the scalar diquark binding disappears.

IV. INSTANTON-INDUCED INTERACTION IN DENSE MATTER

A. Quark Zero Modes

In the previous section the instanton-induced interactions between quarks were approximated by effective *local* 4-fermion vertices. In the microscopic treatment of sect. II, the external quarks couple to the quark zero modes in the instanton field, leading to a *nonlocal* profile function for the interaction vertex with a size characterized by the typical instanton radius of about $\rho=0.33$ fm. In dense matter at zero temperature, the single-instanton solution itself is not affected by the surrounding quarks. The zero-mode wave functions, however, *are* density dependent leading to important modifications of the instanton-induced interactions in the medium. They can be constructed from the Dirac equation at finite (quark-) chemical potential,

$$(i \not{D}_I - i\mu\gamma_4)\phi_I = 0 . \quad (28)$$

The correct solution was obtained in [33,34]:

$$\phi_I = i \frac{\rho}{2\pi} \frac{e^{\mu t}}{x} \sqrt{\rho^2 + x^2} \not{\partial} \frac{[\cos(\mu r) + \frac{t}{r} \sin(\mu r)] e^{-\mu t}}{\rho^2 + x^2} \chi_L , \quad (29)$$

where the spinor χ_L arises from an antisymmetric (singlet) coupling of spin and color wave functions, as before. Note that the solution of the adjoint Dirac equation,

$$\phi_I^\dagger(x; -\mu) (i \not{D}_I - i\mu\gamma_4) = 0 , \quad (30)$$

carries the chemical potential argument with opposite sign. This is necessary for a consistent definition of expectation values at finite μ , and in particular renders a finite norm,

$$\int d^4x \phi_I^\dagger(x; -\mu) \phi_I(x; \mu) = 1 , \quad (31)$$

whereas without the extra sign one has

$$\int d^4x \phi_I^\dagger(x; \mu) \phi_I(x; \mu) = \infty . \quad (32)$$

This singularity, corresponding to the particle-particle channel, is in fact directly related to well-known BCS singularity one encounters when resumming an effective (attractive) particle-particle interaction around the Fermi surface (see, e.g., ref. [35]).

B. Instanton Form Factors

Using the explicit form of the zero mode wave function, we calculate the form factor from the Fourier transform

$$\begin{aligned} \tilde{\phi} &= \int d^4x \phi(x) e^{-ik \cdot x} \\ &= 2i\rho \int_0^\infty dR R^3 \int_0^\pi d\eta \sin^2 \eta \int_0^\pi d\theta \sin \theta \frac{e^{\mu t}}{x} \sqrt{\rho^2 + x^2} (\gamma_0 \partial_t + \vec{\gamma} \cdot \hat{k} \cos \theta \partial_r) \\ &\quad \frac{(\cos(\mu r) + \frac{t}{r} \sin(\mu r)) e^{-\mu t}}{\rho^2 + x^2} e^{-i(\omega t + k r \cos \theta)} \chi_L , \end{aligned} \quad (33)$$

where $x^2 = r^2 + t^2$ and $\hat{k} = \vec{k}/k$. Introducing hyper-spherical coordinates for the integration, $r = R \sin \eta$, $t = R \cos \eta$, the result can be expressed through two scalar functions $A(\omega, k, \mu)$ and $B(\omega, k, \mu)$, given in appendix B, as

$$\tilde{\phi} = [\gamma_0 B(\omega, k, \mu) + \vec{\gamma} \cdot \hat{k} A(\omega, k, \mu)] \chi_L \equiv \tilde{\psi} \chi_L , \quad (34)$$

The finite density zero mode wave functions $\tilde{\psi}$ have the symmetry properties

$$\tilde{\psi}(\omega, \vec{k}, \mu) = \tilde{\psi}^*(-\omega, -\vec{k}, \mu) i = \tilde{\psi}^*(\omega, \vec{k}, -\mu) . \quad (35)$$

The combination $\mathcal{F}(\omega, \vec{k}, \mu) = \psi^*(\omega, \vec{k}, \mu) G_0^{-1}(\omega, \vec{k}, \mu)$ appears in the effective quark interaction on each propagator entering or exiting the instanton-induced vertex. In the mean field approach, when two of the propagators participating in the vertex have the same momentum, it is useful to combine them into two new formfactors. For a propagator entering the instanton vertex and another exiting with the same momentum one obtains

$$\alpha = \mathcal{F}(-\omega, -\vec{k}, \mu)^\dagger \mathcal{O} \mathcal{F}(\omega, \vec{k}, \mu), \quad (36)$$

where \mathcal{O} is a matrix with Dirac, color and flavor indices. For an overall unit matrix, one has

$$\begin{aligned} \alpha &= (\gamma_0 i(\omega - i\mu) + i\vec{\gamma} \cdot \vec{k})(\gamma_0 B^*(\omega, k, \mu) + \vec{\gamma} \cdot \hat{k} A^*(\omega, k, \mu))^2 \\ &\quad (\gamma_0 i(\omega - i\mu) + i\vec{\gamma} \cdot \vec{k}) \\ &= (A^{*2} + B^{*2})(k^2 + (\omega - i\mu)^2) \\ &\equiv \alpha_r + i\alpha_i. \end{aligned} \quad (37)$$

For a propagator entering the instanton vertex and a transposed one exiting with the same momentum one finds

$$\beta = \mathcal{O} \mathcal{F}(-\omega, -\vec{k}, \mu)^T \mathcal{O} \mathcal{F}(\omega, \vec{k}, \mu). \quad (38)$$

When the Dirac part of \mathcal{O} is $C\gamma_5$, where C is the charge conjugating matrix,

$$\begin{aligned} \beta &= C\gamma_5(\gamma_0^T i(-\omega - i\mu) - i\vec{\gamma}^T \cdot \vec{k})(\gamma_0^T B^*(-\omega, k, \mu) - \vec{\gamma}^T \cdot \hat{k} A^*(-\omega, k, \mu)) \\ &\quad C\gamma_5(\gamma_0 B^*(\omega, k, \mu) + \vec{\gamma} \cdot \hat{k} A^*(\omega, k, \mu))(\gamma_0 i(\omega - i\mu) + i\vec{\gamma} \cdot \vec{k}) \\ &= (\gamma_0(\omega + i\mu) + \vec{\gamma} \cdot \vec{k})(\gamma_0 B(\omega, k, \mu) + \vec{\gamma} \cdot \hat{k} A(\omega, k, \mu)) \\ &\quad (\gamma_0 B^*(\omega, k, \mu) + \vec{\gamma} \cdot \hat{k} A^*(\omega, k, \mu))(\gamma_0(\omega - i\mu) + \vec{\gamma} \cdot \vec{k}) \\ &= (\omega^2 + k^2 + \mu^2)(|A|^2 + |B|^2) + 2\mu k i(A^* B - AB^*) \\ &\quad + i\gamma_0 \vec{\gamma} \cdot \hat{k} [2\mu k(|A|^2 + |B|^2) + (\omega^2 + k^2 + \mu^2)i(A^* B - AB^*)] \\ &\equiv \beta_r + i\gamma_0 \vec{\gamma} \cdot \hat{k} \beta_i. \end{aligned} \quad (39)$$

We note that α and β have the same symmetry as in Eq. (35).

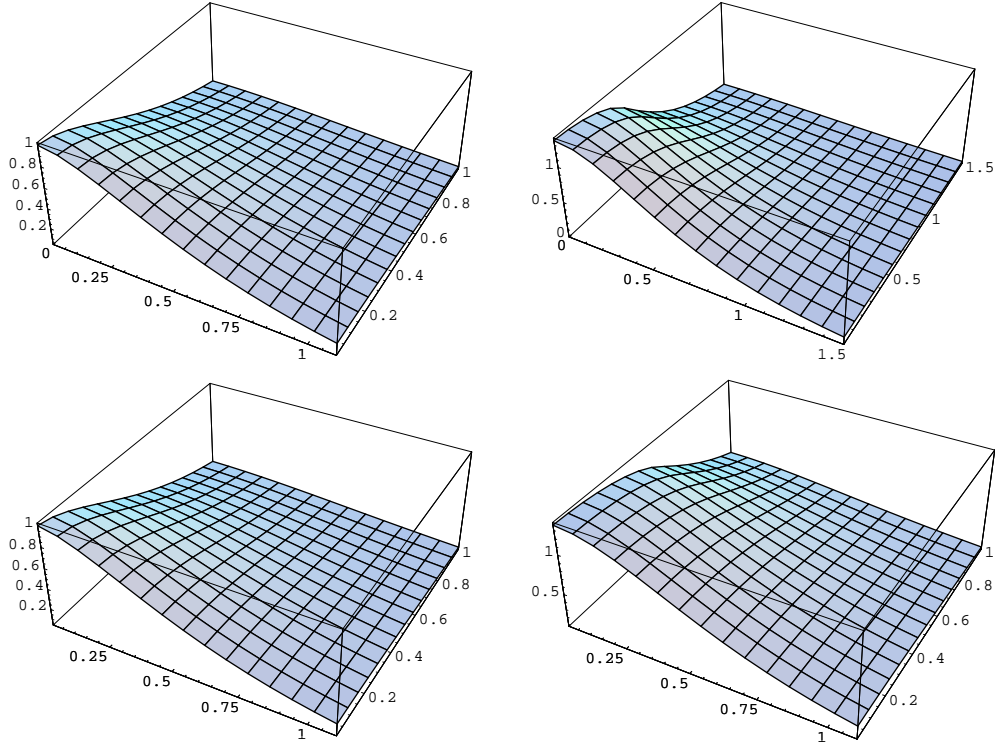


FIG. 2. The moduli squared of the form factors, $|\alpha|^2 = \alpha_r^2 + \alpha_i^2$ (top panels) and $|\beta|^2 = \beta_r^2 - \beta_i^2$ (bottom panels), for two different values of the chemical potential: $\mu = 0$ (left column) and $\mu = 300$ MeV (right column).

C. Quark Overlap Matrix Elements

The instanton formfactors discussed above are designed for momentum space calculations, in particular for extracting effective interactions between quarks in the mean-field framework. However, in the statistical mechanics treatment of the instanton liquid partition function presented in sect. VIII, the coordinate space description is the more suitable one. For that we will need the explicit form of the fermionic overlap matrix element T_{IA} which at finite density takes the form

$$\begin{aligned} T_{IA}(z, u; \mu) &= \int d^4x \phi_I^\dagger(x - z_I; -\mu) (i \not{D} - i\mu\gamma_4) \phi_A(x - z_A; \mu) \\ &= - \int d^4x \phi_I^\dagger(x - z_I; -\mu) (i \not{\partial} - i\mu\gamma_4) \phi_A(x - z_A; \mu) . \end{aligned} \quad (40)$$

The second line is again obtained by virtue of the Dirac equation when choosing the sum ansatz for the gauge-field configurations, $A_\mu = A_\mu^I + A_\mu^A$. T_{IA} plays a crucial role in the fermionic determinant of the instanton partition function, where it generates the fermionic interaction ('quark hopping amplitude') between I 's and A 's and is therefore responsible for correlations in the instanton liquid. In particular, T_{IA} controls the probability of forming molecules.

The definite chirality of the zero modes (in the limit of vanishing current quark masses) entails that I - I and A - A matrix elements are zero. In the vacuum Lorentz invariance implies that the overlap matrix element can be characterized by a single scalar function [36], *e.g.*, $T_{IA} \equiv i u \cdot \hat{z} f(z)$. In the medium this is no longer true and T_{IA} must be calculated in terms of two independent scalar functions f_1, f_2 according to

$$T_{IA}(z, u; \mu) \equiv i u_4 f_1(\tau, r; \mu) + i \frac{(\vec{u} \cdot \vec{r})}{r} f_2(\tau, r; \mu) . \quad (41)$$

They are shown in Fig. 3, see also [37,38]. Similar to the finite temperature case, we observe a strong enhancement with increasing μ in the temporal direction. Moreover, the fermionic interaction becomes very long range, $\sim \mu^2/x_4$ (at finite temperature it was limited to the Matsubara box of size $1/T$ enforced by periodic boundary conditions). In the spatial direction, the exponential damping $\exp[-\pi T r]$ in the finite- T case is replaced by oscillations $\sim \sin(\mu r)$. The latter also effectively suppress the hopping amplitude once the r -integration in the partition function is performed.

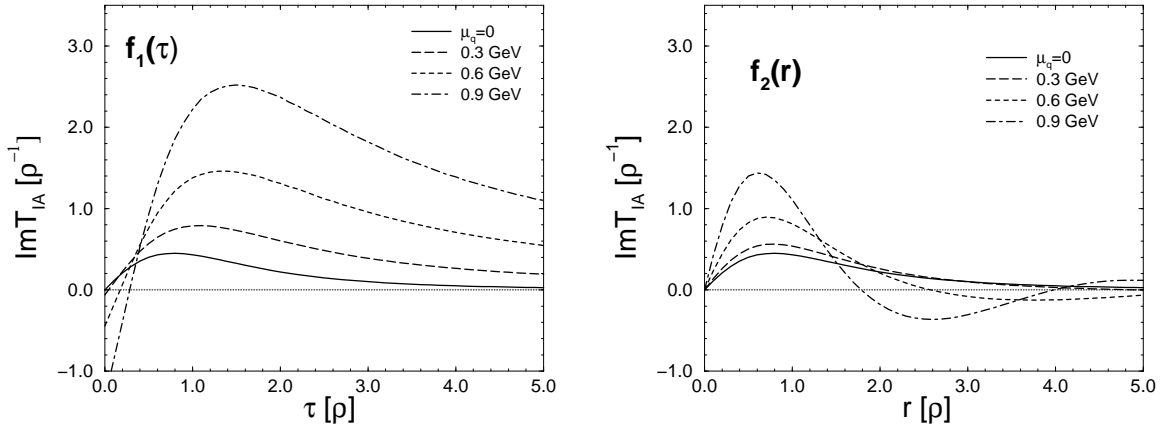


FIG. 3. Quark-induced I - A -interaction at finite density for the most attractive color orientation $u_4=1$, $\vec{u}=0$ as well as $r=0$ (left panel) and for $u_4=0$, $|\vec{u}|=1$ and $\tau=0$ (right panel).

From the strong enhancement of T_{IA} with increasing μ one may already anticipate the relevance of molecule configurations at finite densities [37]. This issue will be quantitatively investigated in the 'cocktail' model in sect. VIII.

V. THE TWO-FLAVOR PROBLEM

This section will be devoted to study finite density two-flavor QCD in the mean-field approximation using the exact momentum dependent instanton profile functions as discussed in sect. IV B. As density increases the basic competition

will be between the chiral condensate $\langle \bar{q}q \rangle$ and the scalar ud diquark condensate in the $\langle qq \rangle$ channel, representing the color superconducting state as discussed in Refs. [2,1]. We will first discuss the corresponding coupled gap equations formalism (sect. V A) and then proceed to the numerical results and their interpretation in sect. V B.

A. Mean-Field Grand Canonical Potential at Finite μ

For the evaluation of the grand canonical potential we employ the Cornwall-Jackiw-Tomboulis (CJT) [39] effective action, which is elucidated in more detail in Appendix C. It involves 3 type of propagators (including their antiparticle pendants) corresponding to single (anti-) quarks carrying color charge that participates in the diquark condensate (G_1, \bar{G}_1), single (anti-) quarks carrying color charge that is not part of the diquark condensate (G_2, \bar{G}_2), and (anti-) diquarks (F, \bar{F}). The minimization of the action with respect to (*w.r.t.*) these propagators generates the following six gap equations:

$$\begin{aligned} &-(G_1 - F\bar{G}_1^{-1}\bar{F})^{-1} + G_0^{-1} - M_1\alpha = 0 \\ &-(\bar{G}_1 - \bar{F}G_1^{-1}F)^{-1} + \bar{G}_0^{-1} + M_1\alpha^* = 0 \\ &-G_2^{-1} + G_0^{-1} - M_2\alpha^* = 0 \\ &-\bar{G}_2^{-1} + \bar{G}_0^{-1} + M_2\alpha^* = 0 \\ &\bar{G}_1^{-1}\bar{F}(G_1 - F\bar{G}_1^{-1}\bar{F})^{-1} + i\Delta\beta = 0 \\ &G_1^{-1}F(\bar{G}_1 - \bar{F}G_1^{-1}F)^{-1} + i\Delta\beta^* = 0, \end{aligned} \quad (42)$$

where

$$\begin{aligned} M_1 &= 2g \left(\frac{1}{8N_c^2} (\text{tr}(G_1 + G_2)\alpha) + \frac{1}{\sqrt{2}} \frac{N_c - 2}{16N_c^2(N_c^2 - 1)} (\text{tr}\lambda_8(G_1 + G_2)\alpha) \right), \\ M_2 &= 2g \left(\frac{1}{8N_c^2} (\text{tr}(G_1 + G_2)\alpha) - \frac{2}{\sqrt{2}} \frac{N_c - 2}{16N_c^2(N_c^2 - 1)} (\text{tr}\lambda_8(G_1 + G_2)\alpha) \right), \\ \Delta &= 2g \frac{1}{8N_c^2(N_c - 1)} \text{tr}(FC\gamma_5\lambda_2\tau_2\beta), \end{aligned} \quad (43)$$

are the two chiral masses and the diquark gap, and G_0 (\bar{G}_0) is the bare (anti-) quark propagator defined through Eq. (C2). As before, the traces involve momentum integrations. The chiral masses are linear combinations of the $\bar{q}q$ condensates, $\text{tr}(G_1\alpha)$ and $\text{tr}(G_2\alpha)$, while the gap Δ is proportional to the qq condensate, $\text{tr}(FC\gamma_5\lambda_2\tau_2\beta)$. Eqs. (43) represent a coupled system of gap equations in the chiral and diquark masses, M_1, M_2 and Δ . To determine their solutions, one needs to know the explicit form of the propagators G_1, G_2 and F . They are constructed from the coupled set of Eqs. (42). Using the relation $\bar{G}(p) = -G^T(-p)$ and the transposition property $C\gamma_5\gamma_\mu^T = \gamma_\mu C\gamma_5$, one can rearrange Eqs. (42) into Gorkov-type equations (note that G, F, \bar{F} do not commute) as

$$\begin{aligned} G_2(p) &= G_0(p) + G(p)M_2\alpha(p)G_0(p) \\ G_1(p) &= G_0(p) + G(p)M_1\alpha(p)G_0(p) + F(p)(i\Delta C\gamma_5\lambda_2\tau_2\beta(p)G_0(p) \\ F(p) &= F(p)M_1\alpha^*(p)G_0^T(-p) + G(p)i\Delta\beta^*(p)C\gamma_5\lambda_2\tau_2G_0^T(-p). \end{aligned} \quad (44)$$

A graphic representation of these equations is displayed in Fig. 4.

The Gorkov equations can be solved in algebraic form yielding

$$\begin{aligned} G_2(p) &= (G_0^{-1}(p) - M_2\alpha(p))^{-1} \\ G_1(p) &= (G_0^{-1}(p) - M_1\alpha(p) + \Delta^2\beta^*(p)(G_0^{-1}(-p) - M_1\alpha^*(p))^{-1}\beta(p))^{-1} \\ F(p) &= i\Delta G_1(p)\beta^*(p)(G_0^{-1}(-p) - M_1\alpha^*(p))^{-1}C\gamma_5\lambda_2\tau_2 \\ &= i\Delta(G_0^{-1}(p) - M_1\alpha(p))^{-1}\beta^*(p)G_1(-p)C\gamma_5\lambda_2\tau_2 \\ &\equiv \tilde{F}(p)C\gamma_5\lambda_2\tau_2 \\ \bar{F}(p) &= i\Delta C\gamma_5\lambda_2\tau_2(G_0^{-1}(-p) - M_1\alpha^*(p))^{-1}\beta(p)G_1(p) \\ &= i\Delta C\gamma_5\lambda_2\tau_2G_1(-p)\beta(p)(G_0^{-1}(p) - M_1\alpha(p))^{-1} \\ &\equiv C\gamma_5\lambda_2\tau_2\tilde{\bar{F}}(p). \end{aligned} \quad (45)$$

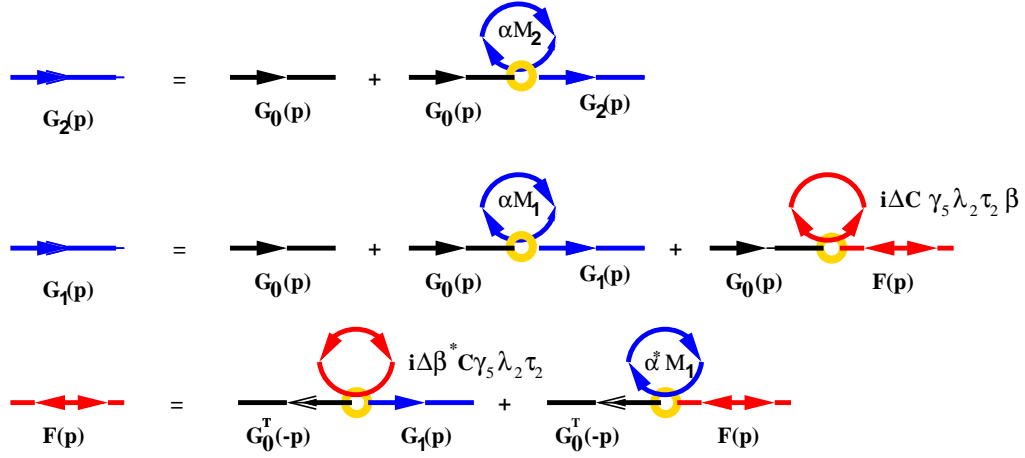


FIG. 4. Diagrammatic representation of the Gorkov Eqs. (44).

To obtain the thermodynamic state variables such as pressure and energy density we need to know the explicit dependence of the thermodynamic potential on the mass parameters. This can be achieved by reinserting the explicit solutions of the propagators into the effective action, Eq. (C12), constituting the grand canonical potential times the 4-volume, $-V_4\Omega(M_1, M_2, \Delta)$. For that purpose we evaluate the propagators more explicitly. After some algebra, one can rewrite G_1 from Eq. (45) as

$$\begin{aligned}
 G_1(p) = & \mathbb{1}_2^{color} \otimes \mathbb{1}_2^{flavor} \otimes \left\{ -i\gamma_0 \left[(\omega - i\mu)((\omega + i\mu)^2 + k^2 + \tilde{M}_1^{*2}) \right. \right. \\
 & + (\omega + i\mu)\Delta^2(\beta_r^2 + \beta_i^2) - 2ik\Delta^2\beta_r\beta_i \left. \right] - i\vec{\gamma} \cdot \hat{k} \\
 & \times \left[k((\omega + i\mu)^2 + k^2 + \tilde{M}_1^{*2}) + k\Delta^2(\beta_r^2 + \beta_i^2) + 2i(\omega + i\mu)\Delta^2 \right] \\
 & \left. - \tilde{M}_1 \left[((\omega + i\mu)^2 + k^2 + \tilde{M}_1^{*2}) + \tilde{M}_1^* \Delta^2(\beta_r^2 - \beta_i^2) \right] \right\} \mathcal{D}^{-1},
 \end{aligned} \tag{46}$$

where $\tilde{M}_1(p) = M_1\alpha(p)$, and

$$\begin{aligned}
 \mathcal{D} = & |(\omega - i\mu)^2 + k^2 + \tilde{M}_1^2|^2 + \Delta^4(\beta_r^2 - \beta_i^2)^2 - 8k\mu\Delta^2\beta_r\beta_i \\
 & + 2\Delta^2(\omega^2 + k^2 + \mu^2)(\beta_r^2 + \beta_i^2) + 2|\tilde{M}_1|^2\Delta^2(\beta_r^2 - \beta_i^2).
 \end{aligned} \tag{47}$$

Using the relation (C5) for the Dirac part (tr_D) of the trace-log in the kinetic part of Eq. (C12) (here the trace does not include the momentum integration), one finds

$$\frac{1}{2} \text{tr}_D \ln(-\bar{G}_1 G_1 + \bar{G}_1 F \bar{G}_1^{-1} \bar{F}) = -4 \ln \mathcal{D}, \tag{48}$$

and from Eq. (46),

$$\begin{aligned}
 \text{Re} [\text{tr}_D (G_0^{-1} G_1 - 1)] = & -4 \left[\text{Re} [((\omega + i\mu)^2 + k^2) \tilde{M}_1^2] + |\tilde{M}_1|^4 + \Delta^4(\beta_r^2 - \beta_i^2)^2 \right. \\
 & - 4k\mu\Delta^2\beta_r\beta_i + \Delta^2(\omega^2 + k^2 + \mu^2)(\beta_r^2 + \beta_i^2) \\
 & \left. + 2|\tilde{M}_1|^2\Delta^2(\beta_r^2 - \beta_i^2) \right] \mathcal{D}^{-1},
 \end{aligned} \tag{49}$$

$$\begin{aligned}
 \text{Re} [\text{tr}_D (G_1 \alpha)] = & -\frac{4}{M_1} \left[\text{Re} [((\omega + i\mu)^2 + k^2) \tilde{M}_1^2] + |\tilde{M}_1|^4 \right. \\
 & \left. + |\tilde{M}_1|^2\Delta^2(\beta_r^2 - \beta_i^2) \right] \mathcal{D}^{-1},
 \end{aligned} \tag{50}$$

$$\text{Re} [\text{tr}_D (\bar{F} \beta)] = \frac{4}{\Delta} \left[\Delta^4(\beta_r^2 - \beta_i^2)^2 - 4k\mu\Delta^2\beta_r\beta_i + \Delta^2(\omega^2 + k^2 + \mu^2) \right. \tag{51}$$

$$\left. \times (\beta_r^2 + \beta_i^2) + |\tilde{M}_1|^2\Delta^2(\beta_r^2 - \beta_i^2) \right] \mathcal{D}^{-1}. \tag{52}$$

The analogous quantities involving G_2 and M_2 are obtained from the above by substituting $\Delta \rightarrow 0$, $M_1 \rightarrow M_2$.

Using the above relations our final expression for Ω becomes

$$\begin{aligned}\Omega(M_1, M_2, \Delta) = & \int_0^\infty d\omega \frac{k^2 dk}{2\pi^3} \left\{ -4 \ln \mathcal{D} - 2 \ln |(\omega - i\mu)^2 + k^2 + \tilde{M}_2^2|^2 \right. \\ & - 4 \text{Re} [\text{tr}_D (G_0^{-1} G_1 - 1)] + 8 \frac{\text{Re} [(\omega + i\mu)^2 + k^2 \tilde{M}_2^2] + |\tilde{M}_2|^4}{|(\omega - i\mu)^2 + k^2 + \tilde{M}_2^2|^2} \Big\} \\ & - \frac{g}{18} \left\{ \int_0^\infty d\omega \frac{k^2 dk}{2\pi^3} \text{Re} [\text{tr}_D (2G_1 \alpha + G_2 \alpha)] \right\}^2 - \frac{g}{144} \left\{ \int_0^\infty d\omega \frac{k^2 dk}{2\pi^3} \text{Re} [\text{tr}_D (G_1 \alpha - G_2 \alpha)] \right\}^2 \\ & - \frac{g}{6} \left\{ \int_0^\infty d\omega \frac{k^2 dk}{2\pi^3} \text{Re} [\text{tr}_D (\tilde{F} \beta)] \right\}^2. \end{aligned} \quad (53)$$

The global minimum of Ω *w.r.t.* M_1, M_2, Δ at each μ determines the thermodynamically stable phase and the values of M_1, M_2, Δ are the chiral masses and color superconducting gap in that phase. The extrema of Ω at each μ can be found by equating the derivatives *w.r.t.* M_1, M_2, Δ to zero. Equivalently, one can verify that after differentiating the expression for Ω *w.r.t.* M_1, M_2 and Δ one recovers Eqs. (43). Their solutions correspond to the local extrema of Ω and represent different possible phases. We shall discuss them in the next subsection. Phase transitions correspond to two distinct minima of Ω having an equal value (first order), or merging together (second order).

One should recall that in this fomulation the coupling constant g is an integration variable: an inverse Laplace transformation was used to exponentiate the instanton vertex. However, in the thermodynamic limit the saddle-point approximation for the g -integration becomes exact (since it is multiplied by the 4-volume V_4). Identifying the potential energy of Ω in Eq. (53) as $-gU$, the integral in question is

$$\mathcal{Z} \propto \int dg \exp[-gU + \frac{N}{V} \ln(g)], \quad (54)$$

where N/V is the total instanton density. The saddle point is then found to be at

$$g_{max} = \frac{N}{V} \frac{1}{U}. \quad (55)$$

Thus, at the saddle point the new potential energy is $-N/V \ln(U)$, up to a constant.

The real question is how to determine the μ dependence of N/V . This will be addressed in sect. VIII within a statistical mechanics treatment taking into account correlations in the instanton ensemble. It will be shown there that the simplifying assumption of a constant total instanton density is indeed reasonably justified. Another approximation concerns the density-dependence of the second key parameter, the average instanton radius ρ , which defines the scale in all instanton calculations. Lacking better knowledge, we also assume that it does not vary significantly at the chemical potentials under consideration.

B. $N_f = 2$ Phase Diagram

Solutions of the gap equations are extrema of Ω , but only minima represent a thermodynamic phase. There are 4 types of solutions to (43):

1. There is a chiral condensate, but no diquark one, *i.e.*, $M_1 = M_2 = M, \Delta = 0$,
2. There is a diquark condensate, but no chiral one, *i.e.*, $M_1 = M_2 = 0, \Delta \neq 0$,
3. Both condensates are present, *i.e.*, all $M_1, M_2, \Delta \neq 0$,
4. No condensates at all, *i.e.*, $M_1 = M_2 = \Delta = 0$.

The last case corresponds to free quarks and it is easy to see that, at $T = 0$, having at least one condensate is always more favorable. The rather complicated expressions for the formfactors require the integrals in Eq. (43), together with Eq. (55), to be evaluated numerically for each value of μ varying from 0 to 500 MeV. We shall call the three types of solutions described above phase 1, 2 and 3, and fix our two input numbers as $\rho = 1/3$ fm and $(N/V)\rho^4 = 0.0116$, corresponding to $N/V = 0.94$ fm⁻⁴.

With these values we find that at $\mu = 0$ the system is in phase 1 with the familiar value of about 330 MeV for the chiral mass M at $\mu = 0$. We normalize the grand-canonical potential such that the minimum at $\mu = 0$ has zero

pressure, $\Omega = 0$. We find minima for phase 1 in the range of μ from 0 to 360 MeV, for phase 2 for all values of μ and for phase 3 only for values of μ between 250 and 290 MeV. The values of Ω for all three phases are shown in Fig. 5.

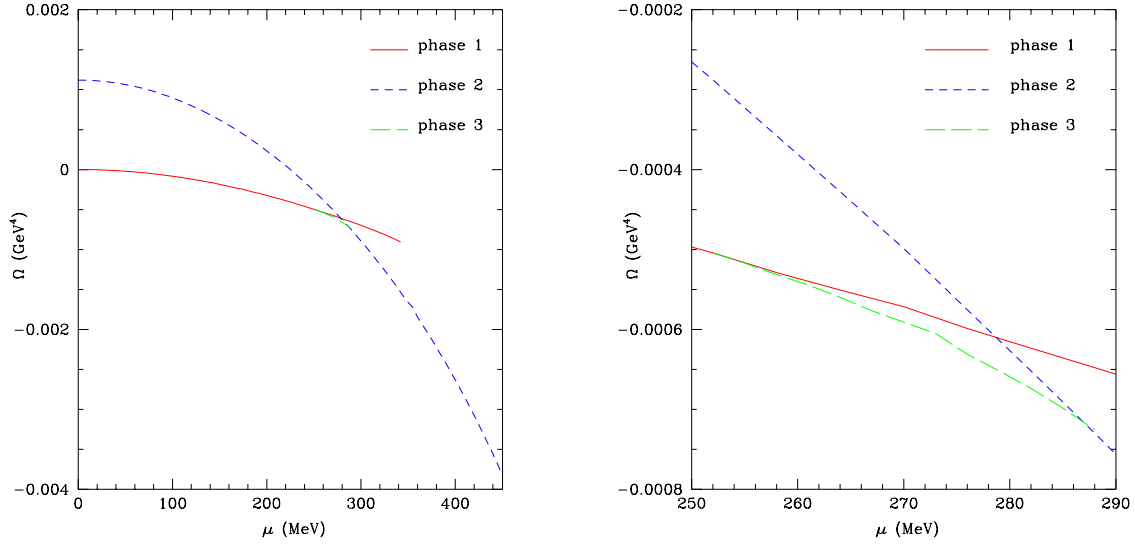


FIG. 5. Ω for phases 1, 2 and 3. The right panel is a magnification of the region between 250 and 290 MeV, where phase 3 exists.

Phase 1 dominates until 250 MeV where the system makes a transition to phase 3, and then, at 288 MeV, there is a transition to phase 2. The coupling constant g for all three phases changes little (not shown). The mass M for phase 1, the gap Δ for phase 2 and the two masses M_1, M_2 and the gap Δ for phase 3 are shown in Fig. 6.

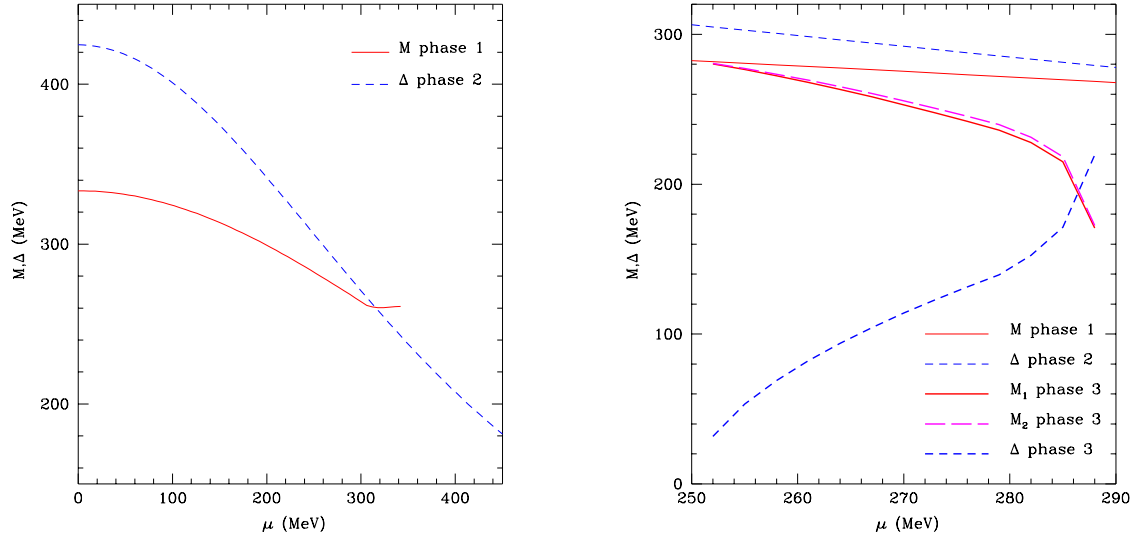


FIG. 6. The left panel shows M for phase 1 and Δ for phase 2. The right panel is a magnification of the region between 250 and 290 MeV, with the masses and gaps of all three phases.

To understand the nature of the phase transitions we study the dependence of Ω on the three parameters M_1, M_2 and Δ . As seen in the right panel of Fig. 6, phase 3 starts at the values of the masses and the gap of phase 1 at $\mu = 250$ MeV. This is an indication of a second order phase transition, as the corresponding chiral and diquark condensates (which are proportional to M_1, M_2 and Δ) are the first derivatives of Ω *w.r.t.* these masses and the gap. The emergence of the phase transition at $\mu = 250$ MeV is exhibited even more clearly in the left panel of Fig. 7.

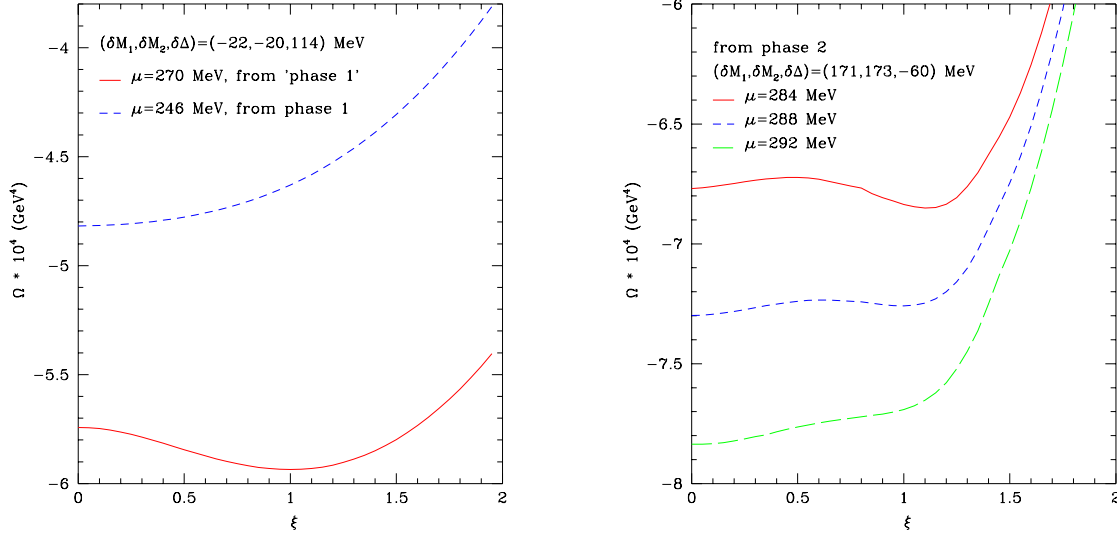


FIG. 7. The left panel shows profiles of Ω at $\mu = 270$ and 246 MeV along the direction that at $\mu = 270$ MeV connects the solution for phase 1 ($\xi = 0$) and phase 3 ($\xi = 1$). The right panel shows Ω at $\mu = 284$, 288 and 292 MeV along the direction that at $\mu = 288$ MeV connects the solution for phase 1 ($\xi = 0$) and phase 3 ($\xi = 1$).

At $\mu = 270$ MeV, we have plotted the values of Ω on a straight line in the parameter space ($M_1 = M_{1,ph1} + \xi\delta M_1$, $M_2 = M_{2,ph1} + \xi\delta M_2$, $\Delta = \Delta_{ph1} + \xi\delta\Delta$), connecting phase 1 ($\xi = 0$) with phase 3 ($\xi = 1$). We see that the solution for phase 1 is not a minimum but a local maximum of Ω . The second curve shows Ω just before the transition, where phase 3 has not yet emerged, but the minimum is quite flat indicating that the second derivative of Ω is close to 0. When moving along the same direction $(\delta M_1, \delta M_2, \delta\Delta)$ in the parameter space we see a classic example of a second order phase transition, when at certain value of the parameter μ the symmetry changes (the SU(3) color symmetry is broken to SU(2)), a diquark condensate appears, the second derivative of Ω goes through 0 and the old solution (with the higher symmetry) turns from a minimum into a maximum. The new absolute minimum is phase 3. Of course any new extrema can only turn up in pairs, but all solutions are symmetric *w.r.t.* the sign of Δ so that the two new minima must be at $\pm\Delta$.

The second phase transition at $\mu = 286$ MeV is analyzed in the right panel of Fig. 7. The middle curve shows the values of Ω at $\mu = 270$ MeV on a straight line in the parameter space ($M_1 = M_{1,ph2} + \xi\delta M_1$, $M_2 = M_{2,ph2} + \xi\delta M_2$, $\Delta = \Delta_{ph2} + \xi\delta\Delta$), connecting phase 2 ($\xi = 0$) with phase 3 ($\xi = 1$). At this value of μ phase 2 already dominates over phase 3. The opposite situation is observed from the upper curve which is for $\mu = 284$ MeV with the cross-section of Ω in the same direction in the parameter space. Obviously a first order phase transition occurs for some μ between these two values. However, the barrier between the phases is quite low and the values of the parameters (M_1, M_2, Δ) (and the condensates) of the two phases are quite close, so it is a rather weak first order transition. This is further supported by the fact that at $\mu = 290$ MeV the minimum for phase 3 disappears quite rapidly (by going through an inflection point), as seen from the right panel of Fig. 7. For the lowest curve only phase 2 exists, but the remnant of the inflection point is visible.

There are some shortcomings in the mean-field analysis as presented here. Below some critical μ_c , which marks the onset transition, no physical quantity should depend on μ . Due to the fact that the instanton zero modes explicitly depend on μ – however small – this is not respected in our calculation. Nevertheless, the variation of M and Ω below the phase transition is quite small. The result might be further improved by taking into account the dependence of the instanton density and size on μ . Another problem is that the onset transition happens quite early, at $\mu \simeq 250$ MeV, whereas the expected onset corresponds to a third of the nucleon mass minus the binding energy of nuclear matter $(939 - 16)/3 \text{ MeV} \simeq 308$ MeV. Again, this might be related to various approximations employed.

It is interesting to note that we do find all three phases to exist, not just the chirally broken and superconducting phases, but also a phase with chiral symmetry breaking and diquark condensation. The existence of the latter phase is not a very firm prediction as the difference in energy density of the three phases in the transition regions is rather small. In fact, phase 3 was not observed in the NJL calculation of [5] or the instanton calculation of [37] or [13]. The latter work uses slightly different techniques to evaluate the grand canonical potential. We will return to the (speculative) phase with simultaneous diquark condensation and chiral symmetry breaking in the discussion in sect. IX B.

VI. THREE FLAVOR QCD IN THE CHIRAL LIMIT

The situation becomes more involved if one includes the strange quark. Since the critical chemical potential $\mu_c \sim 300 - 350$ MeV is larger than the strange quark mass $m_s \simeq 140$ MeV, strange quarks have to be included whenever there is time for strangeness to equilibrate. There are several qualitatively new features in going from $N_f = 2$ to $N_f = 3$. First, since $N_f = N_c$, there are new order parameters in which the color and flavor orientation of the condensate is locked [3]. Second, the instanton-induced interaction is a six-fermion vertex, so it does not directly induce the BCS instability.

In this section we will consider $N_f = 3$ flavor QCD in the chiral limit. In that case, we expect that in the low density phase chiral symmetry is broken by a quark condensate $\langle \bar{u}u \rangle = \langle \bar{d}d \rangle = \langle \bar{s}s \rangle$. In the high density phase, quark pairs are condensed. One possible form of ordering is the analog of the $N_f = 2$ diquark condensate, $\langle q_i^a C \gamma_5 q_j^b \rangle = \Delta_c^k \epsilon_{ijk} \epsilon_{abc}$. This order parameter breaks color $SU(3)_C \rightarrow SU(2)_C$ and the chiral $SU(3)_L \times SU(3)_R \rightarrow SU(2)_L \times SU(2)_R$. A more attractive possibility is provided by the following order parameter [3]

$$\langle q_{i,R}^{a\alpha} q_{j,R}^{b\beta} \rangle = \frac{1}{2} (C^\dagger \gamma_5 P_R)^{\alpha\beta} (\Delta_1 \delta_{ia} \delta_{jb} + \Delta_2 \delta_{ib} \delta_{ja}). \quad (56)$$

Here, P_R is the projector on right-handed quark fields, and there is an analogous expression for left-handed fields also. This order parameter breaks color and chiral symmetry down to the diagonal subgroup $SU(3)_{C+L+R}$. Since the color symmetry is completely broken, there is a gap in the spectrum for all 9 quarks and 8 gluons. This already suggests that the phase characterized by Eq. (56) should be preferred over the $N_f = 2$ like phase, in which only 4 quark states are gaped. We will see this more explicitly in the next section.

The order parameter (56) breaks chiral symmetry since the residual symmetry couples flavor rotations of right and left handed quarks. The diagonal symmetry acts on the quark fields as

$$q_i^a \rightarrow (U^*)_{ij} U^{ab} q_j^b, \quad (57)$$

where U is an element of $SU(3)$. The most general form of the quark condensate that is consistent with this symmetry is

$$\langle \bar{q}_{L,i}^{a\alpha} q_{R,j}^{b\beta} \rangle = \frac{1}{2} (P_R)^{\alpha\beta} \left(\left(\Sigma_0 - \frac{2}{3} \Sigma_8 \right) \delta^{ab} \delta_{ij} + 2 \Sigma_8 \delta_i^a \delta_j^b \right). \quad (58)$$

At zero density we expect Σ_8 to be zero, but in the high density phase both Σ_0 and Σ_8 will in general be non-zero.

It is important to note that even though the above argument establishes that chiral symmetry is broken, it does not show how a chiral condensate is actually formed. From the superfluid order parameter (56), we can directly form the chiral order parameter $\langle (\bar{q}_L q_R)^2 \rangle \sim \langle \bar{q}_L \bar{q}_L \rangle \langle q_R q_R \rangle$, but not the chiral condensate $\langle \bar{q}_L q_R \rangle$. This is because (56) violates right (and left) handed quark number by two units, whereas $\langle \bar{q}_L q_R \rangle$ violates right and left handed quark number by one unit. In other words, the order parameter leaves a discrete chiral symmetry unbroken, and this symmetry prevents the quark condensate from acquiring an expectation value. But this discrete symmetry is explicitly broken by instantons. In the color-flavor-locked phase, we can saturate four of the external legs of the instanton vertex $(\bar{q}_L q_R)^3$ with the condensate and obtain an effective interaction $\langle \bar{q}_L \bar{q}_L \rangle \langle q_R q_R \rangle \langle \bar{q}_L q_R \rangle$ which leads to the formation of a quark condensate.

In the case of three massless flavors, the 't Hooft interaction is a flavor antisymmetric six-fermion interaction [41–43]

$$\begin{aligned} \mathcal{L} = G_6 (2\pi\rho)^6 \frac{1}{6N_c(N_c^2 - 1)} \epsilon_{f_1 f_2 f_3} \epsilon_{g_1 g_2 g_3} & \left(\frac{2N_c + 1}{2N_c + 4} (\bar{\psi}_{L,f_1} \psi_{R,g_1}) (\bar{\psi}_{L,f_2} \psi_{R,g_2}) (\bar{\psi}_{L,f_3} \psi_{R,g_3}) \right. \\ & \left. + \frac{3}{8(N_c + 2)} (\bar{\psi}_{L,f_1} \psi_{g_1}) (\bar{\psi}_{L,f_2} \sigma_{\mu\nu} \psi_{R,g_2}) (\bar{\psi}_{L,f_3} \sigma_{\mu\nu} \psi_{R,g_3}) + (L \leftrightarrow R) \right). \end{aligned} \quad (59)$$

In the following, we will consider the somewhat more general case of a $U(1)_A$ violating six-fermion interaction characterized by two independent coupling constants $G_{6,1}$ and $G_{6,2}$, corresponding to the scalar and tensor terms in Eq. (59).

In the vicinity of the Fermi surface, six-fermion terms are suppressed *w.r.t.* four-fermion interactions. This is the Cooper phenomenon: Near the Fermi surface, the only interaction that is not suppressed is $2 \rightarrow 2$ scattering, where the two particles are back-to-back. In the more modern language of the renormalization group one finds that the strength of the six-fermion interaction is reduced as one integrates out states away from the Fermi surface [44–46]. In the context of the mean-field approximation employed here, we will see that the gap equation has a logarithmic enhancement in the case of four-fermion interactions, but not for six- (or even higher) fermion vertices.

For this reason we will have to consider the effect of four-fermion interactions. We already stressed that instanton-antiinstanton pairs provide a four-fermion interaction for any number of flavors. In terms of left- and right-handed fermions, the interaction is

$$\mathcal{L}_4 = G_4 \left\{ \frac{2}{N_c^2} [(\bar{\psi}_L \gamma_\mu \psi_L)^2 + (\bar{\psi}_R \gamma_\mu \psi_R)^2] - \frac{1}{N_c(N_c - 1)} [(\bar{\psi}_L \gamma_\mu \lambda^a \psi_L)^2 + (\bar{\psi}_R \gamma_\mu \lambda^a \psi_R)^2] \right. \\ \left. - \frac{4}{N_c^2} (\bar{\psi}_L \gamma_\mu \psi_L)(\bar{\psi}_R \gamma_\mu \psi_R) - \frac{2(2N_c - 1)}{N_c(N_c^2 - 1)} (\bar{\psi}_L \gamma_\mu \lambda^a \psi_L)(\bar{\psi}_R \gamma_\mu \lambda^a \psi_R) \right\}. \quad (60)$$

In the following, we shall study the condensates (56) and (58) for an interaction given by the sum of the four-fermion vertex (60) and the six-fermion vertex (59). In this section, we will consider the coupling constants G_4 and G_6 to be arbitrary parameters, constrained mainly by the known value of the quark condensate at zero density. In sect. VIII E we shall try to determine these couplings from the partition function of the instanton liquid.

The system of gap equations for the three-flavor case can be derived along the same lines as the two-flavor case discussed in the previous section. However, the resulting equations are algebraically much more involved. In order to keep the presentation reasonably simple, we will ignore the instanton form-factors and take the interaction to be point-like. As we saw in the last section in the case of $N_f = 2$, this approximation does not qualitatively affect the results.

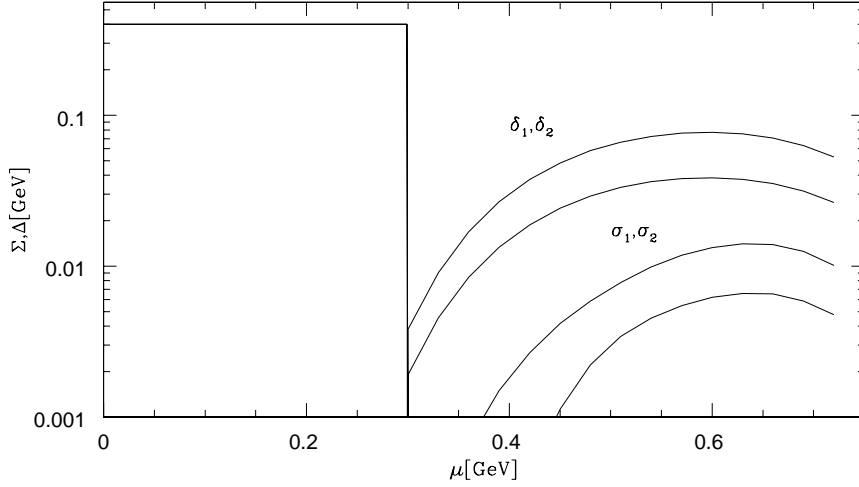


FIG. 8. Chiral and superconducting gaps $\sigma_{1,2}$ and $\delta_{1,2}$ as a function of the chemical potential for the three-flavor model in the chiral limit.

We shall calculate the thermodynamic potential in the mean-field approximation. This calculation is somewhat complicated by the fact that the color-flavor structure of the propagators is quite involved. The first step is to determine the quadratic part of the action in the mean-field approximation. For this purpose, we close off all except two legs of the interaction. The result is

$$\mathcal{M} = (\bar{q}_{L,i}^a q_{R,j}^b) \left\{ (\delta^{ab} \delta_{ij}) \left[G_4 \left(\frac{16}{3} \Sigma_0 - \frac{2}{9} \Sigma_8 \right) + G_{6,1} \left(84 \Sigma_0^2 + 8 \Sigma_0 \Sigma_8 - \frac{74}{3} \Sigma_8^2 + \frac{9}{2} \Delta_A^2 \right) \right. \right. \\ \left. \left. + G_{6,2} \left(144 \Sigma_0^2 + 48 \Sigma_0 \Sigma_8 - 168 \Sigma_8^2 - 30 \Delta_A^2 \right) \right] \right. \\ \left. + (\delta_i^a \delta_j^b) \left[G_4 \frac{2}{3} \Sigma_8 + G_{6,1} \left(-24 \Sigma_0 \Sigma_8 + 10 \Sigma_8^2 - \frac{3}{2} \Delta_A^2 \right) \right. \right. \\ \left. \left. + G_{6,2} \left(-144 \Sigma_0 \Sigma_8 + 120 \Sigma_8^2 + 18 \Delta_A^2 \right) \right] \right\} \\ + (q_{R,i}^a C \gamma_5 q_{R,j}^b) \left\{ (\delta_i^a \delta_j^b - \delta_j^a \delta_i^b) \Delta_A \left[\frac{2}{3} G_4 + G_{6,1} (3 \Sigma_0 - 2 \Sigma_8) + G_{6,2} 12 (3 \Sigma_0 - 4 \Sigma_8) \right] \right\}. \quad (61)$$

We note that the interaction is only sensitive to the antisymmetric part $\Delta_A = \Delta_1 - \Delta_2$ of the $\langle qq \rangle$ order parameter. This is different from the OGE interaction considered in [3], but does not make much of a difference in practice, since even in that case the solution of the gap equation has $\Delta_S/\Delta_A \ll 1$, where $\Delta_S = \Delta_1 + \Delta_2$. We also note that there is a chiral symmetry breaking $\bar{q}q$ interaction proportional to Δ_A^2 . This is as expected: Color-flavor-locking combined with instantons leads to chiral symmetry breaking. We also stress that both ingredients, instantons and color-flavor-locking, are essential.

The $\langle qq \rangle$ and $\langle \bar{q}q \rangle$ mass terms can be diagonalized simultaneously. In general, the mass term can be decomposed as

$$(\bar{q}_{L,i}^a q_{R,j}^b) \{g_0 M_0 + g_1 M_1\} + (q_{R,i}^a C \gamma_5 q_{R,j}^b) \{f_1 M_1 + f_2 M_2\} , \quad (62)$$

where we introduced the color-flavor matrices

$$M_0 = \delta^{ab} \delta_{ij}, \quad M_1 = \delta_i^a \delta_j^b, \quad M_2 = \delta_j^a \delta_i^b . \quad (63)$$

The matrices M_1, M_2, M_3 commute. This means that there is a color-flavor basis in which (62) becomes diagonal. We denote the quark fields in this basis by ϕ_ρ , with $\rho = 1, \dots, 9$. The mass term becomes

$$\left(\sum_{\rho=1}^8 \{ \sigma_1 (\bar{\phi}_{\rho,L} \phi_{\rho,R}) + \delta_1 (\phi_{\rho,R} C \gamma_5 \phi_{\rho,R}) \} \right) + \{ \sigma_2 (\bar{\phi}_{9,L} \phi_{9,R}) + \delta_2 (\phi_{9,R} C \gamma_5 \phi_{9,R}) \} , \quad (64)$$

where $\sigma_1 = g_0$, $\delta_1 = -f_2$ is eightfold degenerate and $\sigma_2 = g_0 + 3g_1$, $\delta_2 = 3f_1 + f_2$. In our case

$$\begin{aligned} \sigma_1 = G_4 \left(\frac{16}{3} \Sigma_0 - \frac{2}{9} \Sigma_8 \right) + G_{6,1} \left(84 \Sigma_0^2 + 8 \Sigma_0 \Sigma_8 - \frac{74}{3} \Sigma_8^2 + \frac{9}{2} \Delta_A^2 \right) \\ + G_{6,2} \left(144 \Sigma_0^2 + 48 \Sigma_0 \Sigma_8 - 168 \Sigma_8^2 - 30 \Delta_A^2 \right) \end{aligned} \quad (65)$$

$$\begin{aligned} \sigma_2 = G_4 \left(\frac{16}{3} \Sigma_0 + \frac{16}{9} \Sigma_8 \right) + G_{6,1} \left(84 \Sigma_0^2 - 64 \Sigma_0 \Sigma_8 + \frac{16}{3} \Sigma_8^2 \right) \\ + G_{6,2} \left(144 \Sigma_0^2 - 384 \Sigma_0 \Sigma_8 + 192 \Sigma_8^2 + 24 \Delta_A^2 \right) \end{aligned} \quad (66)$$

$$\delta_1 = \frac{1}{2} \delta_2 = \Delta_A \left(\frac{2}{3} G_4 + G_{6,1} (3 \Sigma_0 - \Sigma_8) + G_{6,2} (-3 \Sigma_0 + 4 \Sigma_8) \right) . \quad (67)$$

The potential for the mean field is given by closing of all external legs of the interaction. This way we get two-loop graphs proportional to G_4 and three-loop graphs proportional to G_6 . In the mean-field approximation, we have

$$\begin{aligned} V = G_4 \left(2 \Delta_A^2 + 12 \Sigma_0^2 + \frac{8}{3} \Sigma_8^2 \right) + G_{6,1} \left(504 \Sigma_0^3 - 384 \Sigma_0 \Sigma_8^2 + \frac{320}{3} \Sigma_8^3 + 24 (3 \Sigma_0 - 2 \Sigma_8) \Delta_A^2 \right) \\ + G_{6,2} \left(864 \Sigma_0^3 - 2304 \Sigma_0 \Sigma_8^2 + 1280 \Sigma_8^3 - 144 (3 \Sigma_0 - 4 \Sigma_8) \Delta_A^2 \right) . \end{aligned} \quad (68)$$

In the quadratic part of the interaction we can now integrate over the fermion fields. Since the color-flavor structure is already diagonal, we get a sum of nine terms, each (in principle) with different gap parameters. We finally obtain the following result for the free energy

$$F = -8\epsilon(\sigma_1, \delta_1) - \epsilon(\sigma_2, \delta_2) + V . \quad (69)$$

Here, the single particle energy is given by

$$\epsilon(\sigma, \delta) = \int \frac{d^3 p}{(2\pi)^3} \left\{ \sqrt{(E_p - \mu)^2 + \delta^2} + \sqrt{(E_p + \mu)^2 + \delta^2} \right\} , \quad (70)$$

and $E_p^2 = p^2 + \sigma^2$. The mean-field parameters $\Sigma_0, \Sigma_8, \Delta_A$ are determined by making the free energy stationary $(\partial F)/(\partial \Sigma_i) = (\partial F)/(\partial \Delta_i) = 0$. This gives three coupled gap equations that have to be solved numerically.

Before we present the results we have to discuss how to fix the coupling constants G_4 and G_6 . We take $G_{1,2}$ to have the relative size implied by the instanton interaction (59). If we were to ignore random instantons, and only had instanton-antiinstanton pairs, the four-fermion interaction would break chiral symmetry for $G_4 > 7.5 \Lambda^{-2}$. We consider this to be the upper limit on this interaction. In order to see how large the gaps in the three-flavor case can

possibly be, we take G_4 just below this limit $G_4 = 7.4\Lambda^{-2}$. G_6 is then fixed by the requirement that for $m_s = 150$ MeV (see next section) we get a reasonable constituent u, d mass of 400 MeV. This gives $G_6 = 12.0\Lambda^{-5}$.

Results for the various gaps are shown in Fig. 8. Note that the superconducting gap is smaller as compared to the two-flavor case. This is because diquark condensation is now due to pairs, not individual instantons, and we restricted the size of the corresponding coupling such that it does not lead to chiral condensation at $\mu = 0$. This is similar to the scenario of Alford et al. [3], where superconductivity for $N_f = 3$ is driven by one-gluon exchange. Again, reason dictates that the corresponding coupling is below the critical coupling for chiral condensation.

Instantons lead to chiral condensation in the diquark condensed phase. This is immediately clear because if we take the six-fermion vertex and close off four legs by two diquark insertions, the remaining interaction violates chiral symmetry. Color-flavor locking is nevertheless essential. For the two-flavor superfluid order parameter, instantons only lead to a non-zero $\langle \bar{s}s \rangle$. Alford et al. realized that chiral symmetry would be broken, but could not calculate the size of the effect in their model. Here we find it to be very small. The maximum constituent mass generated in the diquark condensed phase is less than 10 MeV. Qualitatively, this is not hard to understand: the constituent mass arises from terms in (61) that are proportional to Δ_A^2 . These terms arise as exchange terms from the original interaction (59), so they are suppressed by degeneracy factors $2N_f N_c$. In addition to that, the constituent mass is driven by the superconducting gap squared, which is already about an order of magnitude smaller than the zero density chiral gap.

There is one more important direct instanton effect in the high density phase. For $N_f = 3$ all chirally invariant four-fermion interactions (molecules, OGE, etc.) are $U(1)_A$ invariant, and do not distinguish between scalar and pseudoscalar diquarks. This means that a parity broken vacuum characterized by the order parameter

$$\langle q_i^a C q_j^b \rangle = \bar{\Delta}_1 \delta_{ia} \delta_{bj} + \bar{\Delta}_2 \delta_{ib} \delta_{ja} \quad (71)$$

is degenerate with the parity conserving vacuum considered here. The same is true for an arbitrary linear combination of positive and negative parity condensates. The degeneracy is lifted by the six-fermion interaction in conjunction with finite quark masses or non-vanishing chiral condensates. This implies that the difference in energy density between the parity broken and parity conserving vacua is small. This is different from the $N_f = 2$ case, where the four-fermion interaction distinguishes between (71) and (56), and the energy difference is big. This effect is also different from the scenario considered by Pisarski and Rischke [47], who argued that the parity broken vacuum is degenerate with the parity conserving one if instanton effects are small. In three-flavor QCD in the chiral limit parity broken and parity conserving vacua are almost degenerate, even if instanton effects are not small.

VII. FLAVOR SYMMETRY BREAKING

The situation is even more complicated if we take flavor symmetry breaking into account. For simplicity, we will restrict ourselves to $m_u = m_d = 0$ and $m_s \neq 0$. It is clear that as $m_s \rightarrow \infty$, we have to recover the two-flavor scenario, with the order parameter given by

$$\langle q_i^a C \gamma_5 q_j^b \rangle = \Delta_{ud} \epsilon_{ij3} \epsilon^{ab3} . \quad (72)$$

Note that in the two-flavor case the color orientation of the condensate is arbitrary, but for three flavors the choice (72) is preferred because it preserves an $SU(2)$ subgroup of the diagonal $SU(3)_{C+L+R}$. We might also consider additional gap parameters that have a different color orientation, but the corresponding gap equation simply decouples and the solution (except in the limit $m_s \rightarrow \infty$) is not energetically favored.

Since flavor symmetry is broken, the structure of the quark condensate is also more complicated. The following ansatz generalizes Eq. (58):

$$\langle \bar{q}_{L,i}^{\alpha} q_{R,j}^{b\beta} \rangle = \frac{1}{2} (P_R)^{\alpha\beta} \left(\left(\Sigma_0 - \frac{2}{3} \Sigma_8 \right) \delta^{ab} \delta_{ij} + \Sigma_s \delta^{ab} \delta_{i3} \delta_{j3} + 2 \Sigma_8 \delta_i^a \delta_j^b + \Sigma_{8,1} P_1 + \Sigma_{8,2} P_2 \right) , \quad (73)$$

where $P_1 = \delta^{a3} \delta_{i3} \delta^{b3} \delta_{j3}$ and $P_2 = \delta^{a3} \delta_{i3} \delta_j^b + \delta_i^a \delta^{b3} \delta_{j3}$.

There are a number of complications that occur once flavor symmetry is broken, and it is hard to take into account all of these effects at the same time. In the following we will concentrate on the dynamical interplay between a flavor symmetric four-fermion interaction generated by one-gluon exchange or instanton pairs and the flavor symmetry breaking four-fermion vertex that comes from the six-fermion 't Hooft interaction and a strange mass insertion. In addition to that, we have to take into account that there is no pairing between strange and non-strange quarks if the mismatch between the Fermi momenta is too big. The BCS instability arises for pairs with total momentum zero

where both of the individual momenta are on the Fermi surface. This is not possible if the masses are different and the Fermi surfaces are shifted. In the presence of pairing the Fermi surface is not sharp, but smeared out over an energy range given by the gap. This means that pairing between strange and non-strange quarks is suppressed if the mismatch between the Fermi momenta exceeds the gap,

$$m_s^2/(4p_F) > \Delta . \quad (74)$$

Moreover, there is the problem that the color-flavor matrix characterizing the most general diquark mass term does not commute with the color-flavor structure of the $\langle \bar{q}q \rangle$ mass term. This means that we cannot simultaneously diagonalize the two mass terms, and write the free energy in the simple form (53). Instead it seems unavoidable to deal with the full (spin, color, flavor, and $\langle qq \rangle$ versus $\langle \bar{q}q \rangle$) matrix structure of the quark propagator. On the other hand, we found that, except possibly in a small regime, quark and diquark condensates do not coexist below the critical chemical potential, and that the quark condensate in the high density phase is small. In the following we will therefore treat the quark condensate in the high density phase as a small perturbation.

The important new ingredient if $m_s \neq 0$ is the presence of a four-fermion interaction which operates exclusively in the u, d quark sector. This interaction arises from the 't Hooft interaction, Eq. (59), by closing off two external legs by a strange mass insertion. The result is

$$\begin{aligned} \mathcal{L} = G_6(m_s\rho)(2\pi\rho)^4 \frac{1}{2N_c(N_c^2 - 1)} \epsilon_{f_1 f_2} \epsilon_{g_1 g_2} \left\{ \frac{2N_c - 1}{2N_c} (\psi_{L,f_1}^\dagger \psi_{R,g_1}) (\psi_{L,f_2}^\dagger \psi_{R,g_2}) \right. \\ \left. + \frac{1}{8N_c} (\psi_{L,f_1}^\dagger \sigma_{\mu\nu} \psi_{R,g_1}) (\psi_{L,f_2}^\dagger \sigma_{\mu\nu} \psi_{R,g_2}) + (L \leftrightarrow R) \right\} , \end{aligned} \quad (75)$$

which (of course) has the form of the $N_f = 2$ 't Hooft interaction, but with a coupling constant controlled by the parameter $3m_s/(4\pi^2\rho^2)$. So, unlike in the OGE-based works, the value of the strange quark mass has not just kinematical but also dynamical significance.

Our model then consists of a flavor symmetric four-fermion interaction, the flavor symmetry breaking four-fermion interaction (75), and the flavor symmetric six-fermion interaction (59). In order to compare with work of ARW [1], we take the flavor symmetric four-fermion interaction to be one-gluon exchange. We could equally well have used the instanton-antiinstanton induced interaction – qualitatively this makes very little difference.

In this model, the mass term becomes

$$\begin{aligned} \mathcal{M} = (\bar{q}_{L,i}^a q_{R,j}^b) \left\{ \left(\delta^{ab} \delta_{ij} \right) \left[\frac{16}{3} K \Sigma_0 + (7G_{4,1} + 6G_{4,2}) \Sigma_0 + (84G_{6,1} + 144G_{6,2}) (\Sigma_0^2 + \Sigma_0 \Sigma_s) \right] \right. \\ \left. + (\delta^{ab} \delta_{i3} \delta_{j3}) \left[m_s + \frac{16}{3} K \Sigma_s - (7G_{4,1} + 6G_{4,2}) \Sigma_0 - (84G_{6,1} + 144G_{6,2}) \Sigma_0 \Sigma_s \right] \right\} \\ + (q_{R,i}^a C \gamma_5 q_{R,j}^b) \left\{ (\delta_i^a \delta_j^b) \left[\frac{K}{3} (2\Delta_A - \Delta_S) \right] + (\delta_j^a \delta_i^b) \left[-\frac{K}{3} (2\Delta_A + \Delta_S) \right] \right. \\ \left. + (\epsilon^{3ab} \delta_{3ij}) \left[\frac{4}{3} K \Delta_{ud} + \frac{1}{2} (G_{4,1} - 12G_{4,2}) (\Delta_A + 2\Delta_{ud}) \right] \right\} . \end{aligned} \quad (76)$$

The quark mass term is already diagonal, while the diquark mass term is of the form

$$(q_{R,i}^a C \gamma_5 q_{R,j}^b) \left\{ f_1 M_1 + f_2 M_2 + f_3 M_3 \right\} \quad (77)$$

with $M_{0,1,2}$ as before and $M_3 = \epsilon^{3ab} \epsilon_{3ij}$. This mass matrix has four eigenvalues,

$$\delta_1 = \pm f_2 \quad (78)$$

$$\delta_2 = \pm(f_2 - f_3) \quad (79)$$

$$\delta_{3,4} = \frac{1}{2} \left(3f_1 + 2f_2 + f_3 \pm \sqrt{9f_1^2 + 2f_1 f_3 + f_3^2} \right) , \quad (80)$$

with degeneracies $d_i = 4, 3, 1, 1$. The free energy is given by $F = -\sum_i d_i \epsilon(\sigma_i, \delta_i) + V$ as before, where the potential is

$$\begin{aligned} V = 16K \left(3\Sigma_0^2 + 2\Sigma_0 \Sigma_s + \Sigma_s^2 \right) + 6 \left(7G_{4,1} + 6G_{4,2} \right) \Sigma_0^2 + \left(504G_{6,1} + 864G_{6,2} \right) \Sigma_0^2 (\Sigma_0 + \Sigma_s) \\ + 4K \left(3\Delta_A^2 - 3\Delta_S^2 + 4\Delta_{ud}^2 + 4\Delta_A \Delta_{ud} \right) + \left(G_{4,1} - 12G_{4,2} \right) (\Delta_A + 2\Delta_{ud})^2 . \end{aligned} \quad (81)$$

An important difference as compared to the flavor symmetric case is that we have to take into account the kinematic restriction discussed above. In channels that involve pairing between strange and non-strange quarks we restrict the integration to the regime $(E_p - \mu)^2 > (m_s^2/(4p_F) - \delta^2)$. For a more detailed discussion, we refer the reader to [48] and [49]. Again, the gap equation follows from the requirement that F is stationary *w.r.t.* the gap parameters Σ_i and Δ_i .

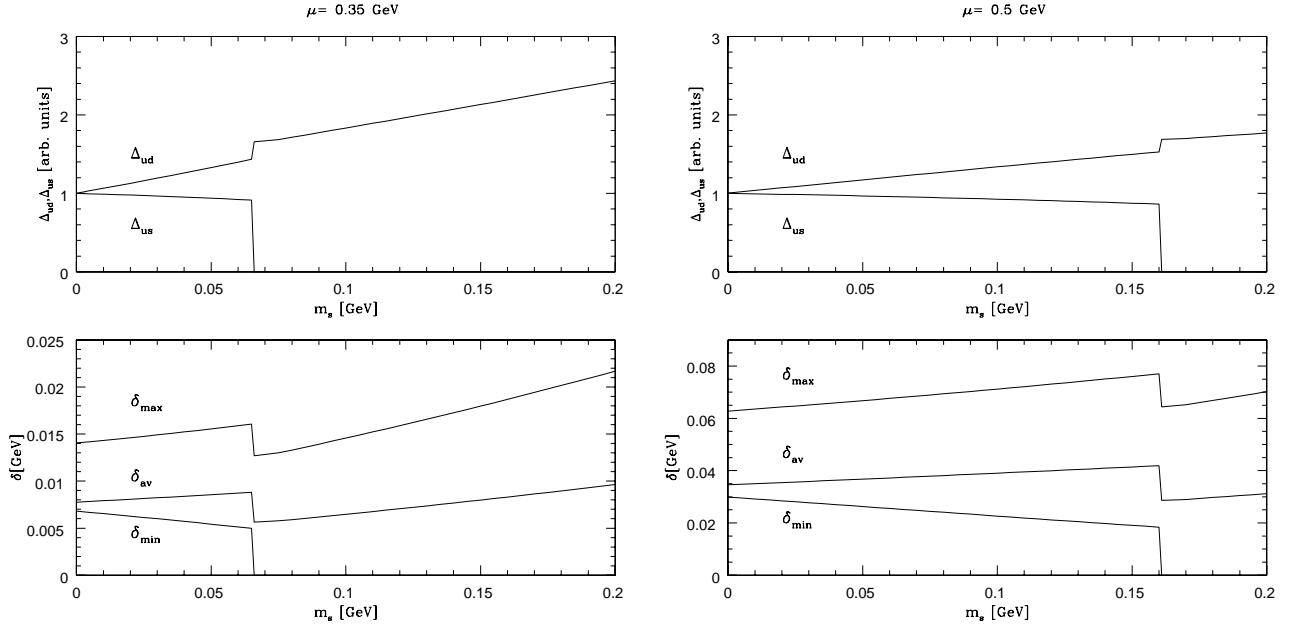


FIG. 9. Superfluid order parameters and gaps as a function of m_s for $\mu = 350$ MeV (left panel) and $\mu = 500$ MeV (right panel). The upper panels show the up-down and up-strange components Δ_{ud} and Δ_{us} of the color-flavor locked state. The lower panels show the maximum, minimum, and average superconducting gap.

Numerical results are shown in Fig. 9. The parameters were fixed as described in the last section. In the figure we plot Δ_{ud} and Δ_{us} as a function of m_s for two different chemical potentials $\mu = 0.35$ and 0.5 GeV. In particular we show the value of the largest, the smallest, as well as the average gap. In the two-flavor case, the smallest gap is zero and the average gap is $4/9$ of the maximum gap. In the three-flavor case, the smallest gap is $1/2$ and the average gap $5/9$ of the maximum gap.

We observe that there is a sharp transition between the two-flavor scenario ($\Delta_{us} = 0, \Delta_{ud} \neq 0$) and the three-flavor scenario ($\Delta_{ud} = \Delta_{us} \neq 0$) that takes place around the physical value of the strange quark mass, $m_s^{crit} = 65$ MeV for $\mu = 0.35$ GeV, and $m_s^{crit} = 160$ MeV for $\mu = 0.5$ GeV. The ratio Δ_{ud}/Δ_{us} grows roughly linearly already for small m_s . This is different from the results of [48,49], and an instanton effect. As discussed above, instantons induce a four-fermion interaction among light quarks which is proportional to m_s . We should note that we have not included the possibility of a dynamically generated contribution to the strange quark mass in the superfluid phase. In terms of the current mass, this effect will shift the critical mass to smaller values.

VIII. STATISTICAL MECHANICS OF THE INSTANTON LIQUID

A. The Cocktail Model at non-zero Density

In this section we take a step beyond the mean-field approximation in that we allow for possible clustering effects in the instanton ensemble. This is achieved by employing a somewhat different formalism. In the previous sections we started from an effective quark interaction obtained by integrating out the gluonic (instanton-) fields in the underlying partition function. In this section we reverse the strategy and integrate over the fermion (quark) fields first. This leads to the following partition function for the instanton ensemble at finite density:

$$\mathcal{Z}_{inst}(\mu) = \sum_{N_+, N_-} \frac{1}{N_+! N_-!} \prod_{I=1}^{N_+, N_-} \int d\Omega_I n(\rho_I) e^{-S_{int}} \rho_I^{N_f} \prod_{f=1}^{N_f} \det(i \not{D} + im_f - i\mu\gamma_4). \quad (82)$$

The original QCD path-integral over all possible gluonic field configurations has been converted into an integration over the collective coordinates $\Omega_I = \{z_I, \rho_I, u_I\}$ (position, size and color orientation) of N_+ instantons and N_- antiinstantons. The single-instanton amplitude $n(\rho_I)$ contains the semi-classical tunneling rate (including one-loop quantum corrections), as well as the Jacobian arising from the introduction of collective coordinates. The instanton interactions can be divided into a gluonic part S_{int} and a fermionic part represented by the determinant of the Dirac operator. It is usually approximated in the subspace of zero modes, *i.e.*,

$$\det(i \not{D} - i\mu\gamma_4) \simeq \det \begin{pmatrix} 0 & T_{IA}(\mu) \\ T_{AI}(\mu) & 0 \end{pmatrix}, \quad (83)$$

where T_{IA} is the fermionic overlap matrix element discussed in sect. IV C, see Eq. (40). When restricted to the zero mode basis, the fermionic determinant is in fact equivalent to the sum of all closed loop diagrams to all orders in the 't Hooft effective interaction. The non-hermiticity of the finite- μ Dirac operator is reflected by the fact that

$$\begin{aligned} T_{AI}(\mu) &= T_{IA}^\dagger(-\mu) \\ &\neq T_{IA}^\dagger(\mu), \end{aligned} \quad (84)$$

i.e., the fermionic determinant is complex, entailing the well-known 'sign'-problem in the partition function, which will be addressed below.

In the statistical mechanics treatment chosen here, spontaneous chiral symmetry breaking in the vacuum is generated by randomly distributed uncorrelated anti-/instantons which allow for a delocalization of the associated quark quasi-zero modes corresponding to the formation of a nonzero $\langle q\bar{q} \rangle$ condensate state. In other words, quarks can travel arbitrarily long distances by randomly jumping from one instanton to another (antiinstanton), and thus may carry their chiral charge to spatial infinity where it effectively becomes 'lost'.

In this picture chiral restoration can in principle proceed in two ways: either instantons disappear altogether, or they rearrange into some *finite* clusters which do no longer support any finite $\langle q\bar{q} \rangle$ condensate. In the limit of very large temperature or density instantons will eventually disappear, because Debye screening of the large gluon fields inside the instantons leads to a strong suppression of the tunneling rate. Nevertheless, in the case of finite temperature QCD it was argued [26] that this cannot be the relevant mechanism for chiral restoration, since lattice simulations have observed the transition at rather low temperatures of $T_c^x \simeq 150$ MeV. This, in turn, led to the suggestion that chiral restoration proceeds through the formation of *I-A* molecules. Further support for this idea is provided by lattice measurements of the instanton density at finite temperatures, showing no depletion below T_c^x and a smooth onset of the expected Debye-screening above [16,17]. More recent studies [21,50] seem to find more direct indications for *I-A* molecule formation at $T \approx T_c$, but their quantitative role in the transition remains to be clarified.

At finite density additional possibilities for clustering of the (chirally asymmetric) random instanton liquid into chirally symmetric configurations are available. In particular, random instantons can be supported by diquark condensates for $N_f = 2$ or by a combination of diquark and quark-antiquark ones for larger N_f . However, as we will show in this section, effects of *I-A* molecule formation may still be an important element in the finite- μ chiral restoration transition, as was shown in Ref. [37]. In some sense this is not really surprising: when both T and μ are sufficiently large so that the all condensates are absent (*i.e.*, in the true QGP phase), *I-A* molecules should constitute the preferred configuration for any remaining instanton component in the system.

To investigate the interplay between the various components in the finite density partition function more quantitatively we resort to the 'cocktail-model' introduced in Refs. [51,26]. Here, the instanton ensemble is decomposed into a mixture of random ("atomic") and "molecular" configurations, which yields a grand canonical partition function of the form

$$\mathcal{Z}_{inst}^{a+m} = \sum_{N_a, N_m} \frac{(z_a V_4)^{N_a}}{N_a!} \frac{(z_m V_4)^{N_m}}{N_m!}. \quad (85)$$

In the thermodynamic limit $V_4 \rightarrow \infty$, and using the Stirling formula, the free energy (thermodynamic potential) becomes

$$\Omega_{inst}^{a+m}(n_a, n_m; \mu) = -\frac{\ln[\mathcal{Z}_{inst}^{a+m}]}{V_4} = -n_a \ln \left[\frac{ez_a}{n_a} \right] - n_m \ln \left[\frac{ez_m}{n_m} \right]. \quad (86)$$

The atomic and molecular 'activities' are [51,26]

$$\begin{aligned}
z_a &= 2 C \rho^{b-4} e^{-S_{int}} \langle T_{IA}(\mu) T_{AI}(\mu) \rangle^{N_f/2} \\
&= 2 C \rho^{b-4} e^{-S_{int}} \left(\frac{n_a}{2} \int d^4 z du [T_{IA}(\mu) T_{AI}(\mu)] \rho^2 \right)^{N_f/2} \\
z_m &= C^2 \rho^{2(b-4)} e^{-2S_{int}} \langle [T_{IA}(\mu) T_{AI}(\mu)]^{N_f} \rangle \\
&= C^2 \rho^{2(b-4)} e^{-2S_{int}} \int d^4 z du [T_{IA}(\mu) T_{AI}(\mu)]^{N_f} \rho^{2N_f} .
\end{aligned} \tag{87}$$

The underlying approximation in this approach is that the values of the hopping amplitudes T_{IA} in each individual configuration are replaced by a product of their mean square values in an uncorrelated ensemble. To establish a connection to the (chiral) quark condensate and constituent mass, one can use the mean-field approximation to express them via the “atomic” density n_a as

$$\langle \bar{q}q \rangle = -\frac{1}{\pi\rho} \left(\frac{3}{2} n_a \right)^{1/2} \tag{88}$$

$$M = -C_M \frac{2}{3} (\pi\rho)^2 \langle \bar{q}q \rangle = -C_M (\pi\rho) \sqrt{\frac{2}{3} n_a} , \tag{89}$$

respectively. In the original work of Ref. [52], where these relations have been first derived, the coefficient $C_M = 1$, leading to an effective quark mass of $M^* \simeq 200$ MeV. The latter is to be understood as the average mass of a constituent quark at finite (euclidean) momentum participating in tunneling processes associated with instantons. With increasing four-momentum M^* is appreciably reduced and therefore does not correspond to the usual constituent quark mass M (defined at zero momentum). We account for this by using $C_M = 2$, yielding $M = 400$ MeV. The minimization of the total Ω over n_a and n_m determines their equilibrium values in the ensemble for given T, μ . The corresponding gap equation for the constituent quark mass is the direct analog of the mean-field equation conjugated to the $\langle \bar{q}q \rangle$ condensate, but expressed in terms of different variables.

For a refined treatment at finite densities we supplement the cocktail model by two additional components. Following the arguments given above, we have to account for the possibility that the random instanton component can become engaged in diquark chains, first observed in numerical simulations of the instanton ensemble in the high-density limit [38]. The pertinent term in the free energy reads

$$\Omega_d(n_d; \mu) = -n_d \ln \left[\frac{e z_d}{n_d} \right] \tag{90}$$

with the associated activity

$$z_d = 2 C \rho^{b-4} e^{-S_{int}} \left(\frac{n_a}{2} \int d^4 z du [T_{IA}(\mu) T_{IA}(\mu)]_{\bar{3}} \rho^2 \right)^{N_f/2} . \tag{91}$$

The subscript “ $\bar{3}$ ” indicates the color projection in some predefined direction characterizing the color vector of the diquark. In the same way that n_a determines the constituent quark mass M , the superconducting gap is related to the density n_d as

$$\Delta = C_\Delta \frac{\pi\rho}{(N_c - 1)} \sqrt{\frac{2}{3} n_d} \tag{92}$$

In analogy to Eq. (89) we use $C_\Delta = 2$, but also perform calculations with $C_\Delta = 1.5$ to assess the inherent uncertainty of this mean-field estimate. Notice that in contrary to Eqs. (87), the fermionic overlap matrix element enters Eq. (91) as $(T_{IA})^2$, which, in fact, causes the z -integration to diverge. This is precisely the BCS-singularity of an attractive interaction in the particle-particle channel, here encountered in coordinate space. The standard procedure to treat this singularity is to start from a new ground state which a priori has the gap built into the fermion propagators, thereby regulating the integrals. The net effect of the gap on the overlap integrals is a damping factor for the intermediate quark propagators, which is delineated in appendix D.

The second refinement consists of including a Fermi sphere of quark-‘quasi-particles’ in the free energy, representing the contribution of quark non-zero modes. The final expression for the thermodynamic potential then becomes

$$\Omega(n_a, n_m, n_d; \mu) = \Omega_{inst}^{a+m+d}(n_a, n_m, n_d; \mu) + \Omega_{quark}^{QP}(M, \Delta; \mu) , \tag{93}$$

where the quark contribution is simply given by

$$\Omega_{quark}^{QP}(M, \Delta; \mu) = \epsilon_q(M, \Delta; \mu) - \mu n_q(M, \Delta; \mu) \quad (94)$$

with

$$\begin{aligned} n_q(M; \mu) &= g_q \int d^3k n_F(\mu - \omega_k) \\ \epsilon_q(M; \mu) &= g_q \int d^3k \omega_k n_F(\mu - \omega_k) , \end{aligned} \quad (95)$$

$g_q = 2N_c N_f$ and $\omega_k^2 = M^2 + k^2$ (in the superconducting phase the dispersion relations of paired quarks picks up an additional dependence on the gap Δ , see below).

At this point it is instructive to compare the 'cocktail model' with other approaches. The (simpler) philosophy employed in the first part of this paper introduces the multi-fermion interactions with a *constant* coupling g , independent of condensates and temperature/density. However, since g is itself generated through instantons, density variations of the latter will affect the coupling. A step towards including this feature was made by Carter and Diakonov [13]: their coupling parameter, called λ (which essentially corresponds to z_a without the fermionic determinant part), was subjected to minimization. The resulting gap equation relates the mean instanton density n_a to λ and the condensates. However, instead of calculating λ and then finding n_a (as done here), they stayed in the mean-field approximation in which the instanton density remains unchanged. Our results to be discussed below support the (approximate) validity of this assumption.

To investigate possible mechanisms for chiral symmetry restoration at finite density in some detail, in particular the competition between diquark and molecule formation, we will in the following separately discuss various versions of the cocktail with increasing complexity, *i.e.*, the two-flavor model including (anti-) instantons, molecules and a Fermi sphere of constituent quarks (sect. VIII B), additionally including the simplest ud -pairing as discussed in Refs. [1,2] (sect. VIII C), and the three-flavor case (sect. VIII D). In sect. VIII E we also give estimates for the density-dependence of effective coupling constants for molecule-induced (anti-)quark-quark interactions, which naturally emerge from the formalism employed in this section.

B. Two Flavor Cocktail Model without Diquark Condensates

In this subsection we basically follow the approach of Ref. [26], generalizing it to finite density [37]. The issue here is to assess the potential role of I - A molecule formation in chiral symmetry restoration at finite density, without the additional complication of superconducting gaps.

For the actual calculations we now have to face the problem of the complex fermionic determinant appearing in the various activities, Eqs. (87) and (91). As has been suggested in Ref. [37], it can be solved under the assumption that the gluonic interaction does not exhibit a pronounced dependence on the color angles, approximating it by an average value (see below). As a result, the color dependence in the activities only enters through the combinations of T_{IA} 's, which then can be integrated analytically, rendering the fermionic determinant real. For two flavors one obtains

$$\begin{aligned} z_a(z_4, r) &\propto \int du T_{IA}(\mu) T_{IA}^\dagger(-\mu) = \frac{1}{2N_c} [f_1^+ f_1^- + f_2^+ f_2^-] \\ z_m(z_4, r) &\propto \int du [T_{IA}(\mu) T_{IA}^\dagger(-\mu)]^{N_f} = \frac{(2N_c - 1) \{f_1^+ f_1^- + f_2^+ f_2^-\}^2 + \{f_1^+ f_2^- - f_1^- f_2^+\}^2}{4N_c(N_c^2 - 1)} \end{aligned} \quad (96)$$

where $f_i^\pm \equiv f_i(\pm\mu)$ are defined through Eqs. (40) and (41). Note that the color averaging of the former complex expressions is sufficient to yield real-valued activities. Also note that, whereas $z_m(z_4, r)$ is a positive definite quantity, this is not the case for $z_a(z_4, r)$ due to the oscillations in $f_{1,2}(r)$. In fact, when further integrating $z_a(z_4, r)$ over space-time (the remaining four collective coordinates), delicate cancellations occur, which require accurate numerical values for the $f_{1,2}^\pm$; otherwise one easily encounters negative/incorrect results for both activities at finite chemical potential. The gluonic interaction entering Eqs. (87) has been approximated by an average repulsion $S_{int} = \kappa \rho^4 (n_a + 2n_m)$, where $\kappa = \beta/2\bar{\rho}^4(N/V)$, $\beta = b/2 + 3N_f/4 - 2$, $b = \frac{11}{3}N_c - \frac{2}{3}N_f$. The free parameter κ characterizes the diluteness of the ensemble. In the case $N_c = 3$ and $N_f = 2$ we have chosen $\kappa \simeq 130$ in order to reproduce the phenomenological value for the diluteness of the instanton vacuum. The normalization constant $C \propto (\Lambda_{QCD})^b$ can also be fixed in the vacuum by requiring that the absolute minimum of the thermodynamic potential $\Omega_{inst}(\mu = 0; n_a, n_m)$ appears at a total instanton density of $N/V = n_a + 2n_m = 1.4 \text{ fm}^{-4}$, being realized for $n_a = 1.34 \text{ fm}^{-4}$ and $n_m = 0.03 \text{ fm}^{-4}$,

which gives $\Lambda_{QCD} \simeq 260$ MeV. The smallness of the molecular component in the vacuum is a consequence of the large entropy associated with quantum fluctuations of the color angles, randomizing the system. Available lattice data agree that such correlations are indeed small at $T = \mu = 0$.

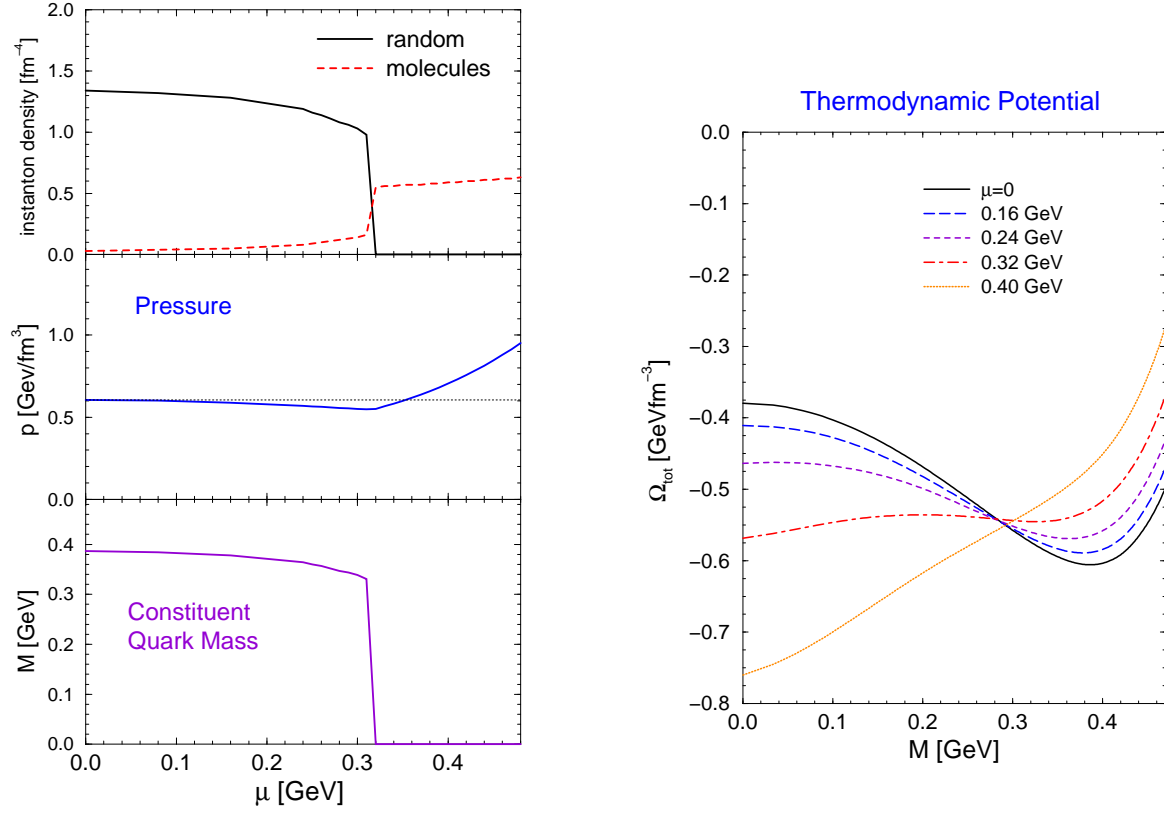


FIG. 10. Results for the two-flavor cocktail model *without* diquark pairing; the left part shows the densities of random instantons ('atomic' component) and I - A molecules (upper left panel), the pressure $p = -\Omega$ (middle left panel) and the constituent quark mass (lower left panel) after minimizing the free energy, Eq. (93), *w.r.t.* n_a and n_m . In the right panel the free energy is displayed as a function of the constituent quark mass $M \propto n_a^{1/2}$, indicating a first order transition from the minimum at finite M to the one at $M = 0$.

Our numerical findings for the $N_c = 3, N_f = 2$ atomic+molecular instanton cocktail model at finite density are summarized in Fig. 10. At small μ essentially nothing happens until, at a critical value $\mu_c \simeq 310$ MeV, the system jumps into the chirally restored phase, the latter being characterized by $n_a = 0$. The transition is of first order, as can be seen by inspection of the M -dependence of the free energy (right panel of Fig. 10). Below μ_c , the pressure actually decreases slightly with increasing μ indicating a mixed phase-type instability, similar to what has been discussed in Refs. [1,53]. The total instanton density at the transition (residing in I - A -molecules) is appreciable, $N/V = 2n_m \simeq 1.1 \text{ fm}^{-4}$, providing the major part of the pressure at this point. In other words: a substantial part of the non-perturbative vacuum pressure persists in the chirally restored phase. The vacuum pressure of $p(\mu = 0) = 0.6 \text{ GeV fm}^{-3}$ (indicated by the dotted line in the middle left panel of Fig. 10) is not recovered until a chemical potential of $\mu_0 = 350$ MeV, corresponding to a free quark number density of $n_q^0 = 1.15 \text{ fm}^{-3}$ (naively, this translates into a nucleon density of $n_N = 2.4n_0$ with the normal nuclear matter density $n_0 = 0.16 \text{ fm}^{-3}$). For all chemical potentials in between, $0 < \mu < \mu_0$, the system is mechanically unstable, possibly indicating droplet formation in the region $M < \mu < \mu_0$ (as suggested in Ref. [1]), where, with a finite quark density, the pressure $p(\mu)$ is below its vacuum value.

A further comment concerning the numerical value of the critical chemical potential, which is very close to a third of the nucleon mass, is in order. Given the various approximations applied it should be regarded as a coincidence. At the same time it most likely provides a *lower* bound for the true value, as has been the case for the finite temperature

calculations of Ref. [20] (resulting in a critical temperature which is about 20% lower than observed on the lattice and might well be related to the fact that the instanton model lacks explicit confinement). On the other hand, the inclusion of superconducting gaps may further reduce the critical chemical potential and in fact dominate the transition, as will be discussed in the following section.

C. Two Flavor Cocktail Model Including Pairing

We now address the effects of diquark condensation. For clarity, let us first ignore the I - A molecule component in the cocktail to study the competition between chiral and diquark condensates only. The additional inclusion of a pairing gap resulting from ud diquark formation at the Fermi surface as discussed in Ref. [2] modifies the quark quasiparticle contribution according to

$$\Omega_q^\Delta(\mu) = \text{tr} \log [D(M, \Delta)] . \quad (97)$$

Here, D denotes the quasiparticle quark-propagator now including the BCS gap Δ . All interaction contributions are effectively accounted for through the instanton part Ω_{inst}^d , cf. Eqs. (90), (91). The resulting expression for the free energy then becomes

$$\Omega(n_a, n_d; \mu) = \Omega_{inst}^{a+d}(n_a, n_d; \mu) + \frac{1}{N_c} [2\Omega_q^\Delta(M, \Delta; \mu) + (N_c - 2)\Omega_q^{QP}(M; \mu)] \quad (98)$$

(the last term accounting for unpaired quarks), which now has to be minimized *w.r.t.* n_a and n_d . The results for two different values of the vacuum instanton density and the (not precisely determined) coefficient C_Δ for calculating the pairing gap (cf. Eq. (92)) are summarized in Tab. I. We find that color superconductivity appears at critical chemical potentials around $\mu_c \simeq 300$ MeV, very similar to the values of the previous section where only I - A molecule formation was considered. The associated gaps range between 120-180 MeV. These results are consistent within 20% with the findings of sect. V and those of Ref. [13]. We should also note that the calculated gaps in our original work [2] are significantly smaller (below ~ 100 MeV) as those were effectively obtained for 2+1 flavors, *i.e.*, in Ref. [2] we included the effect of a reduced (constituent) strange quark mass M_s in the closed-off strange quark loop of the six-fermion instanton vertex, which decreases the effective instanton-induced coupling constant for the four-quark interaction by about 60% in the chirally restored phase. Another feature that emerges here is that the total instanton density changes little across the transition, which a posteriori justifies to assume it as constant in the mean-field calculations of sect. V.

As in the previous section, there is an intermediate constituent quark-diquark phase, similar to what was found in sect. V, but here it again has small negative pressure which makes it mechanically unstable against the formation of a mixed phase.

Let us now turn to the full two-flavor cocktail model with simultaneous account for the chiral and diquark condensates as well as I - A molecules. The total free energy

$$\Omega(n_a, n_d, n_m; \mu) = \Omega_{inst}^{a+d+m}(n_a, n_d, n_m; \mu) + \frac{1}{N_c} [2\Omega_q^\Delta(M, \Delta; \mu) + (N_c - 2)\Omega_q^{QP}(M; \mu)] , \quad (99)$$

is to be minimized *w.r.t.* n_a , n_m and n_d . The results are shown in Fig. 11, using the coefficient of $C_\Delta = 1.5$ in Eq. (92) (which most closely resembles the results of the calculations in sect. V).

$n_a(\mu=0)$ [fm ⁻⁴]	C_Δ	μ_c [MeV]	μ_0 [MeV]	$\Delta(\mu_c)$ [MeV]
1	2	300	355	158
1	1.5	265	290	120
1.4	2	310	375	188
1.4	1.5	270	305	142

TABLE I. Parameter dependence of the critical chemical potential for chiral restoration in a cocktail model with chiral and diquark condensates (no I - A molecules included).

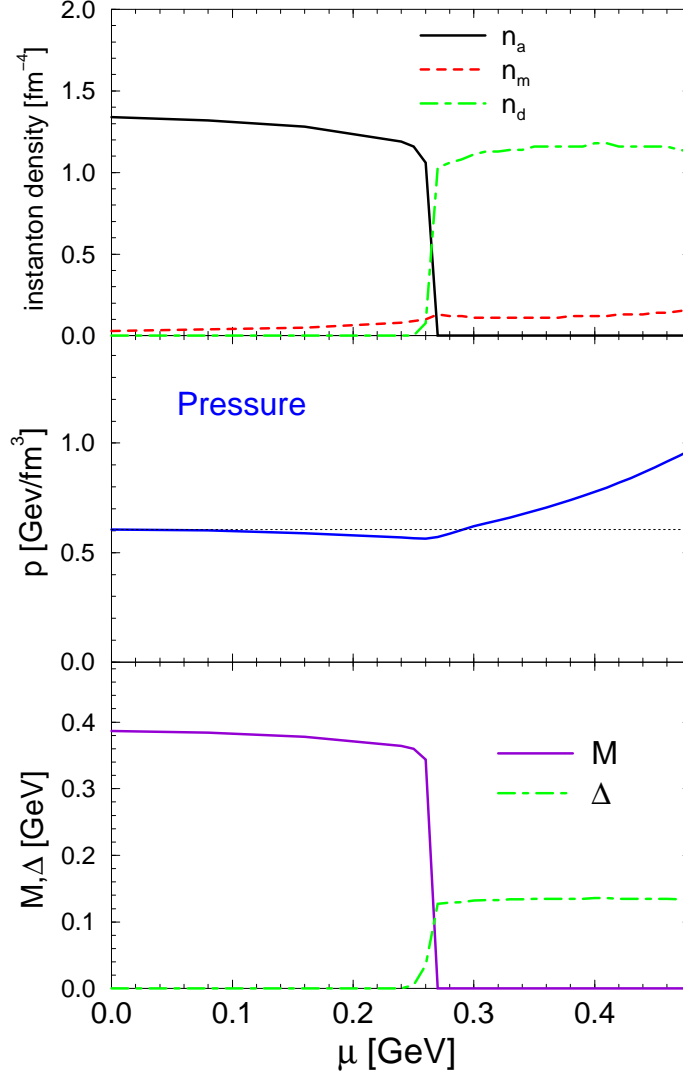


FIG. 11. The full two-flavor cocktail model including I - A molecules and diquark pairing; upper panel: densities of random instantons ('atomic' component, full line), I - A molecules (dashed line) and instantons engaged in 'diquark chains' (dashed-dotted line); middle panel: pressure $p(\mu) = -\Omega(\mu)$, maximized over n_a, n_m and n_d at each value of μ ; lower panel: constituent quark mass (full line, using $C_M = 2$ in Eq. (89) to give $M(\mu = 0) = 400$ MeV) and diquark gap (dashed-dotted line, using $C_\Delta = 1.5$ in Eq. (92), as discussed in the text).

As to be expected from the previous analysis, there is a delicate competition for chiral restoration between random instantons engaged in diquarks and I - A molecule formation. The former do, in fact, induce the chiral transition for all parameter ranges considered.

Towards higher densities it may happen that a second transition occurs within the chirally restored phase characterized by a substantial jump in the molecule density and an accompanied drop of the diquark gap, (its location is somewhat sensitive to parameter choices). The singularity in z_d , on the other hand, guarantees that there is always a finite $\langle qq \rangle$ condensate present, albeit possibly strongly reduced in molecule-dominated phases. In Fig. 11, the transition occurs at $\mu_c = 270$ MeV into a chirally broken diquark phase, which, again, is mechanically unstable. The vacuum pressure is only recovered at $\mu_0 = 295$ MeV, *i.e.*, the combined effect of diquarks and molecules further lowers the μ_0 -values found when including only molecules (Fig. 10, where $\mu_0 = 350$ MeV) or only diquarks (Tab. I, where $\mu_0 = 305$ MeV).

Another important point to note is that the total instanton density, $N/V = n_a + n_d + 2n_m$, is indeed essentially independent of the chemical potential within $\sim 15\%$ or so. *E.g.*, in Fig. 10, the upward jump in the density of molecules is close to half the drop in density of the random instanton component. A similar continuity is seen in Fig. 11 for the more realistic case of the transition between the two kinds of random instanton liquids, associated with the two condensates $\langle \bar{q}q \rangle$ and $\langle qq \rangle$. After all this is not too surprising since, at least for chemical potentials $\mu \leq 0.4$ GeV, the by far dominant fraction of the total energy in the system is carried by the gluonic component residing in instantons, and the free energy itself must of course be continuous across the transition.

Finally, a comment concerning the finite temperature behavior is in order. On the zero-density and finite- T axis it has been shown that molecules drive the chiral restoration. This implies that at finite density, starting from low T , the role of molecules should become more and more relevant; at the same time, color-superconducting gaps are well-known to be suppressed. Thus we expect that for *any* value of μ where there is diquark condensed phase for $T = 0$, a rearrangement into a molecule-dominated phase should occur when raising the temperature. As indicated by our zero temperature results, for chemical potentials $\mu \geq 300$ MeV or so, the corresponding $T_c(\mu)$ line in the phase diagram might actually reach down to fairly low temperatures.

D. Chiral Restoration for more Flavors

As was already mentioned in the introduction, in vacuum the tendency towards chiral restoration in the instanton model strongly increases with the number of flavors, leading to a chirally symmetric vacuum state for N_f as low as ~ 5 . The reason for that has been discussed in sect. II B: the increased number of quark lines enhances the interactions between instantons and antiinstantons, making the random liquid less favorable. More specifically, the integral over color orientations within the molecule, being proportional to $\langle (\cos \theta)^{2N_f} \rangle$, increases more strongly than that for the averaged 'random'-instanton configurations raised to the N_f -th power, $\langle (\cos \theta)^2 \rangle^{N_f}$. The former integral is strongly peaked at $\theta = 0$, creating a "locking" of the color orientation within a molecule.

From continuity one may thus expect that the critical chemical potential for chiral restoration should be further reduced when moving from two to more massless flavors. Here we would like to pursue the question in how far a *third* massless flavor impacts the results of the two-flavor case. For simplicity, we now ignore color superconductivity and consider an interplay between random and molecular components only. As discovered in [3] and further elaborated in the first part of our article, starting from $N_f = 3$ a color-flavor locking phenomenon sets in, leading to a complicated set of $\langle qq \rangle$ and $\langle \bar{q}q \rangle$ condensates. However, they are relatively small in magnitude, and can therefore be neglected for the present purpose.

Compared to the $N_f=2$ case, the color integration for $N_f=3$ is substantially more involved. Using the appropriate relations for the integration over a string of six SU(3)-color matrices (see, *e.g.*, Ref. [54]), one obtains

$$\begin{aligned} z_m(z_4, r) &\propto \int du [T_{IA}(\mu) T_{IA}^\dagger(-\mu)]^{N_f} \\ &= \frac{3(f_1^+ f_1^- + f_2^+ f_2^-)}{16N_c(N_c + 2)(N_c^2 - 1)} \left(3N_c [(f_1^+)^2 (f_1^-)^2 + (f_2^+)^2 (f_2^-)^2] + [4 - N_c] [f_1^+ f_2^- - f_1^- f_2^+]^2 \right). \end{aligned} \quad (100)$$

Note that $z_m(z_4, r)$ in the three-flavor case has no definite sign before integration over space-time (similar to the $N_f=1$ case, *i.e.*, $z_a(z_4, r)$ from Eq. (96)), which inevitably entails partial cancellations. Apparently, only for an even number of flavors the space-time integrand of the finite density activities is positive definite. Performing again the minimization procedure in n_a and n_m for the thermodynamic potential we find that the critical chemical potential is indeed further reduced, by about 10% to $\mu_c \simeq 270$ MeV (as compared to 310 MeV for $N_f=2$). This indeed complies with the above mentioned expectation that at a sufficiently large number of flavors a purely "molecular" vacuum is more preferable than a "random" one, and thus chiral symmetry would be unbroken even in vacuum. As this phenomenon reflects itself also along the μ -axis, we expect μ_c to be further reduced at $N_f=4$, possibly crossing zero at $N_f=5$.

E. Molecule-Induced Effective Couplings

In this section we apply the cocktail model to a microscopic estimate of the density-dependence in the effective coupling constants for (anti-)quark-quark interactions. In the mean-field framework employed in sects. V, VI, VII such density-dependencies were not accounted for.

To begin with let us recall the expression for the effective coupling constant for single-instanton induced interactions as, *e.g.*, used in Ref. [2]:

$$G_{inst} = \int d\rho \, n(\rho, \mu) \, \rho^{N_f} (2\pi\rho)^4, \quad (101)$$

with

$$n(\rho, \mu) = C_{N_c} (8\pi^2/g^2)^6 \exp[-8\pi^2/g(\rho)^2] \, \rho^{-5} \quad (102)$$

denoting the single-instanton distribution, *i.e.*, the semi-classical tunneling amplitude. Replacing the ρ -integration by an average value for $\bar{\rho}$, one has

$$G_{inst} = n^\pm (\bar{\rho})^{N_f} (2\pi\bar{\rho})^4 \quad (103)$$

with the anti-/instanton density n^\pm . Notice that (for $N_f = 2$) six additional powers of ρ appear in the integral of Eq. (101) as compared to the usual expression for the density, $n^\pm = \int d\rho \, n(\rho)$. This entails a significantly larger average value $\bar{\rho}$ than the typical instanton size of about $\rho \simeq 1/3$ fm. In order to be consistent the standard value of the zero-density constituent quark mass $M \simeq 400$ MeV (which requires $G_{inst} \simeq 19.1$ fm²), one should have the effective size saturating this integral to be $\bar{\rho} = 0.51$ fm.

The effective coupling constant for molecule-induced interactions has been first derived in Ref. [28], where it is written as

$$G_{mol} = \int n(\rho_1, \rho_2) \, d\rho_1 \, d\rho_2 \, \frac{1}{T_{IA}^2} (2\pi\rho_1)^2 (2\pi\rho_2)^2 \quad (104)$$

with the total molecule amplitude

$$n(\rho_1, \rho_2) = \int du \, d^4z \, n(\rho_1) \, n(\rho_2) \, T_{IA}(u, z)^{2N_f} \, \rho_1^{N_f} \, \rho_2^{N_f}, \quad (105)$$

which is nothing but the molecular activity given in Eq. (87). The graphical interpretation of Eq. (104) is quite transparent: starting from the molecule amplitude, where *all* $2N_f$ quark legs are closed within the molecule, one 'cuts' open two of them (corresponding to the division by T_{IA}^2) which provides an effective interaction between four external (anti-) quarks. Inserting (105) into (104), and replacing again the size integrals by using average values for $\bar{\rho}$ we obtain

$$G_{mol} = \frac{(2\pi\bar{\rho})^4 \bar{\rho}^{2N_f} n^+ n^-}{8} \int du \, d^4z \, T_{IA}(u, z)^{2N_f-2}. \quad (106)$$

We see that for $N_f = 2$ the individual ρ integrations carry additional powers of ρ^4 , while it is ρ^5 for $N_f = 3$. Those powers should be compared to ρ^6 in Eq. (101) and ρ^0 for the usual instanton density. As these last two integrals lead to $\bar{\rho} \simeq 0.51$ and $1/3$ fm, respectively, we interpolate between them (lacking a more accurate determination of the size distribution), *i.e.*, estimate the appropriate average size values entering Eq. (106) to be $\bar{\rho} \simeq 0.43$ fm for $N_f = 2$ and $\bar{\rho} \simeq 0.47$ fm for $N_f = 3$. The corresponding zero-density values for the coupling constants are (including a factor of 16 accounting for the difference in color coefficients between Eqs. (10) and (12)):

$$\begin{aligned} G_{inst}(\mu = 0, \bar{\rho} = 0.51\text{fm}) &= 19.1 \text{ fm}^2 \\ 16 \, G_{mol}^{N_f=2}(\mu = 0, \bar{\rho} = 0.47\text{fm}) &= 0.86 \text{ fm}^2 \\ 16 \, G_{mol}^{N_f=3}(\mu = 0, \bar{\rho} = 0.43\text{fm}) &= 0.044 \text{ fm}^2. \end{aligned} \quad (107)$$

Obviously, $G_{inst} \simeq 20 \times (16 \, G_{mol}^{N_f=2})$, and $(16 \, G_{mol}^{N_f=2}) \simeq 20 \times (16 \, G_{mol}^{N_f=3})$. Recalling that the fermionic matrix element, averaged over positions and sizes of an I - A -pair, is given by [15]

$$\rho^2 \langle |T_{IA}|^2 \rangle = \frac{2\pi^2}{3N_c} \frac{N\rho^4}{V} \simeq \frac{1}{40} \quad (108)$$

(for $\rho = 1/3$ fm), one readily understands the decreasing magnitudes of the coupling constants in terms of the additional powers of dimensionless diluteness of the ensemble entering Eq. (106). Note that the effect of color

integrations favors molecules, and the corresponding factors compensate, to some degree, powers of the small diluteness parameter.

We are now in position to evaluate the density-dependence of the effective coupling constants. Using the fermionic matrix elements at finite μ , Eq. (40), and performing the color integrations as discussed in sects. VIII B, VIII D we obtain the results shown in Fig. 12; we recall that throughout this paper possible effects from the Debye-screening of instantons at high densities have been ignored. Therefore G_{inst} is in fact a constant as it does not depend on $T_{IA}(\mu)$. On the other hand, the behavior of the molecule-induced couplings depends on the number of flavors: whereas in the $N_f = 2$ case it decreases with μ , the opposite is found for $N_f = 3$. This is directly related to the μ -dependence of the activities calculated in sect. VIII B, since $G_{mol}^{N_f=2}(\mu) \propto T_{IA}^2$ (corresponding to z_a) and $G_{mol}^{N_f=3}(\mu) \propto T_{IA}^4$ (corresponding to $z_m^{N_f=2}$).

It is instructive to compare the values of the coupling constants with the perturbative OGE interaction. For large-angle scattering¹ the coupling is

$$G_{OGE} = \frac{4\pi\alpha_s}{p_{eff}^2}, \quad (109)$$

where p_{eff} is some effective momentum transfer averaged over the Fermi sphere. With $p_{eff} = 0.5 - 1$ GeV and $\alpha_s(p_{eff}) \approx 0.3$ we have $G_{OGE} = 0.15 - 0.7$ fm². This is comparable to the effect of molecules for $N_f = 2$, and significantly larger than that for $N_f = 3$ at low μ . One should note, however, that the structure of the interactions is different. For example, OGE is flavor independent whereas instanton-induced interactions are flavor antisymmetric.

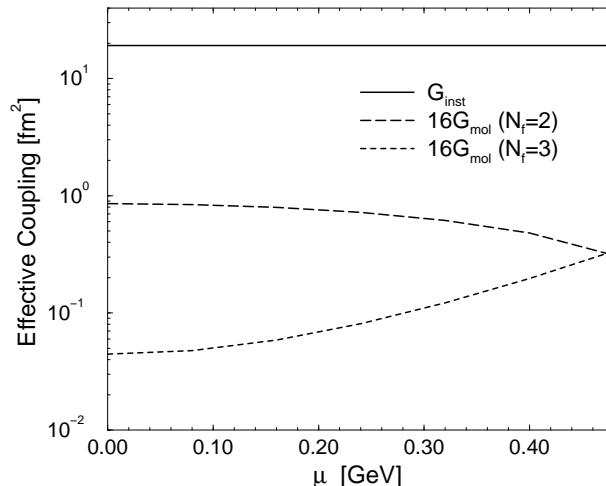


FIG. 12. Instanton-/molecule-induced effective 4-quark coupling constants as a function of chemical potential.

IX. MORE PHASES, OUTLOOK AND EXPERIMENTAL CONSEQUENCES

A. The phase diagram

In this section we would like to put the main results obtained in this work into perspective and discuss the emerging picture of the QCD phase diagram.

The main feature of the phase diagram for two-flavor QCD in the chiral limit and at $T = 0$ is that at a critical chemical potential μ_c the system undergoes a transition from the chirally broken phase to the superconducting

¹For small-angle scattering there appears an additional logarithmic enhancement, which becomes relevant for color superconductivity at asymptotically high μ [11].

phase [1,5,13]. With instanton-induced formfactors we also found a small window in which a chirally broken ‘constituent quark’ plus diquark condensate phase may exist. Unfortunately, this is not a robust prediction of the model, since the free energy differences between the phases are small (in fact, in the cocktail model analysis of sect. VIII this phase is mechanically unstable). We will discuss this issue from a slightly different perspective in the next section.

In any case, the mean-field approach predicts a strong first order phase transition, either from the vacuum phase to superfluid quark matter phase, or from the chirally broken diquark phase to the superfluid phase. This implies the existence of an inhomogeneous phase at intermediate density, with dense quark matter bubbles immersed in the chirally broken phase. Of course, a more refined treatment should reproduce the fact that matter clusters into nucleons and nuclei. In the high density phase chiral symmetry is restored, but color- $SU(3)$ is broken to $SU(2)$. We have not explored the possibility of further breaking $SU(2)$ via color-6 condensates. These condensates seem to generate very small gaps for the up and down quarks of the third color [1].

For three massless flavors we also find a first order phase transition from the chirally broken vacuum phase to the superconducting phase. In spite of the fact that instanton-induced dynamics are very different from OGE considered in Ref. [3], we also find that the preferred order parameter in the superconducting phase exhibits color-flavor-locking. Both color- $SU(3)$ and chiral $SU(3)_L \times SU(3)_R$ are broken, while the diagonal $SU(3)_{C+L+R}$ is preserved. But even though color-flavor locking in general implies that chiral symmetry is broken, instantons are crucial for generating a non-zero value of $\langle \bar{q}q \rangle$. In practice, the value of the chiral condensate turns out to be small.

Furthermore, we have considered the more general case of QCD with 2+1 flavors allowing for a massive strange quark. Of course, the two cases $N_f = 2, 3$ discussed above emerge as limiting cases for $m_s \rightarrow 0$ and $m_s \rightarrow \infty$. For $m_s \simeq 2\sqrt{\Delta\mu}$ pairing between light and strange quarks becomes impossible, and there is a phase transition between the color-flavor locked phase and the two-flavor superconductor. Again, a significant difference between the instanton model and schematic interactions abstracted from one-gluon exchange appears. In the case of OGE, the strange quark mass has a purely kinematical effect. Instantons induce four-fermion interactions of the type $m_s(ud)(\bar{u}\bar{d})$, which can generate large asymmetries between the $\langle ud \rangle$ and $\langle us \rangle = \langle ds \rangle$ components of the color-flavor locked state even for $m_s < m_s^{crit}$. Similar effects are well known from hadronic spectroscopy.

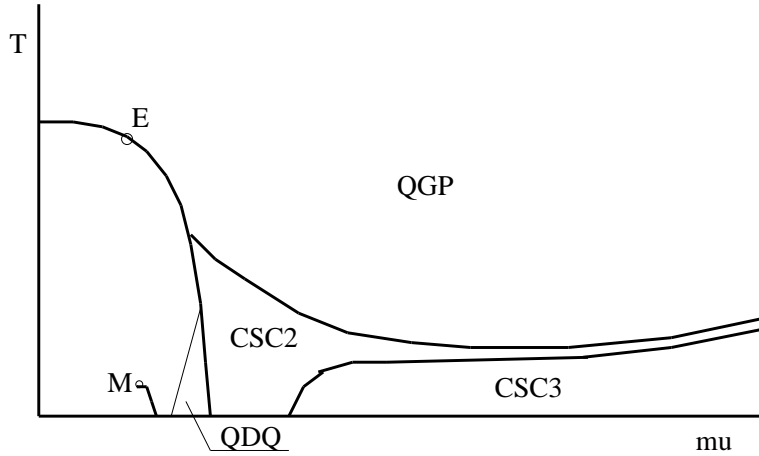


FIG. 13. Schematic QCD phase diagram in the chemical potential μ - temperature T plane. The small T/μ -region corresponds to ordinary hadronic matter, with broken chiral symmetry. The point M (from “multifragmentation”) is the endpoint of the nuclear liquid-gas phase transition. The point E indicates where the first order line either terminates in a second order endpoint (for $m_u, m_d = 0$) or disappears (for finite light quark masses). CSC2 and CSC3 label the $N_f = 2$ and $N_f = 3$ -type superconducting phases. The hypothetical intermediate quark-diquark phase is indicated by QDQ.

In the present work we have not addressed the effects of finite temperature. One would expect that the first order chiral phase transition at $\mu \neq 0$ will persist for some range in temperature, until the transition becomes second order at a tricritical point [6,5]. In BCS theory one can also estimate that superfluidity disappears at a critical temperature $T_c(\mu) \simeq 0.6\Delta(\mu, T = 0)$ (however, as discussed in sect. VIII the impact of instanton-antiinstanton molecules presumably reduces the BCS-coefficient appreciably). As explained above, the boundary between the two types of superconductors should be approximately determined by the condition (74). Since, asymptotically, the gap is expected to slowly grow as a function of chemical potential, the critical temperature will also grow. As a function

of chemical potential the system will eventually reach the color-flavor locked state for any value of the strange quark mass. On the other hand, as a function of temperature (at given μ) one might expect that, since the gap in the two-flavor superfluid is somewhat larger than in the color-flavor locked phase, the system first makes a transition to the two-flavor superconductor, and then to the quark-gluon plasma phase. Combining these conjectures leads to the schematic phase diagram displayed in Fig. 13 (where we have also indicated the nuclear liquid-gas transition line).

B. More Phases?

Finally, we would like to make a few comments on the range of applicability and the limitations of our approach. First, we have restricted ourselves to an instanton model. Even though many of our conclusions apply to any phenomenologically successful effective interaction, many of our numbers are indeed model-dependent.

Furthermore, we have made extensive use of the mean-field approximation (MFA). The MFA is valid provided the condensates are sufficiently smooth, and their fluctuations can be neglected. This assumption becomes better at large density, because in this limit the coupling is weak and Cooper pairs are large compared to the inter-quark distances (as is the case in ordinary superconductors). In the opposite limit of small density the simplest phase one can generate in the mean-field approach is a chirally asymmetric Fermi gas of constituent quarks with masses on the order of 400 MeV. Remarkably enough, our approach predicts that this phase is unstable against separation into a mixed phase, with high density quark droplets separated by pure vacuum [53,1]. While this result appears to be very suggestive, the MFA cannot predict the actual composition of the clusters.

Of course, we know that the “correct” clusters are nucleons. Below nuclear matter saturation density, nucleons themselves will form a mixed phase of clusters (nuclei), but for larger density one has homogeneous nuclear matter. In the vicinity of nuclear saturation density ($n_N = n_0 = 0.16 \text{ fm}^{-3}$), the equation of state is known experimentally. The behavior of the energy density as a function of density is commonly parameterized as

$$\epsilon = (m_N - \delta m_N) n_N + \frac{K n_0}{18} \left(1 - \frac{n_N}{n_0}\right)^2, \quad (110)$$

where $\delta m_N \approx 16 \text{ MeV}$ is the binding energy (per nucleon) of nuclear matter and the compression modulus is on the order of $K^{-1} = 200 - 300 \text{ MeV}$. This means that nuclear matter is rather stiff, that is, the pressure grows very fast as a function of density. The physical reason for the steep rise in pressure is not just Fermi motion, but, more importantly, a strong repulsive core in the nucleon-nucleon interaction. The standard lore is that the steep rise in the pressure with density above saturation density will eventually stop, due to the transition to some other phase of matter, either previously considered scenarios such as pion and kaon condensation [55], or superconducting quark matter. In neutron stars, K^- condensation is additionally favored because of a large electron chemical potential.

Although lacking explicit confinement, the instanton model does provide the interaction to bind quarks into nucleons [30]. The question whether the model provides the repulsive core necessary to prevent nucleons from collapsing into 6 and more quark clusters remains open. Nevertheless, it seems plausible that a sufficiently sophisticated treatment could lead to nuclear matter as the correct ground state at small density.

Can there be other phases, in addition to nuclear matter and superfluid quark matter? In the remainder of this section we will discuss a number of possibilities connected with diquark fluids or Bose condensates. These diquarks would not be Cooper pairs, but tightly bound states. As discussed in sect. III, the instanton model seems to predict such states as bound scalar ud diquarks. The corresponding energy per baryon $E/B = 3M_{dq}/2 \sim 800 - 900 \text{ MeV}$ is lower than the nucleon mass, so it seems natural to look for a diquark phase.

Naively, one would expect diquarks at $T = 0$ to be Bose-condensed in the zero momentum state, because in addition to the gain in binding energy, there is a gain over nuclear or quark matter because no Fermi motion is required. However, since diquarks are colored, this phase could not be color neutral. This means that we have to consider either (i) significant motion of diquarks or (ii) add color-neutralizing quarks.

Let us start with the first idea, with only diquarks at $T = 0$. A good starting point is the question why – if the scalar diquark is bound – a two-baryon state, such as the deuteron, does not decay into a more tightly bound three-diquark state. The simplest color singlet combination of three $(ud)_i = \phi_i$ scalar diquark fields is $\phi_{i1}\phi_{i2}\phi_{i3}\epsilon_{i1,i2,i3}$, but this wave function is antisymmetric, violating Bose statistics. This means that we have to consider p-wave diquark states ϕ_i^m (e.g., in a bag), where m is the third component of angular momentum, in a symmetric combination:

$$\psi = \phi_{i1}^{m1} \phi_{i2}^{m2} \phi_{i3}^{m3} \epsilon^{i1,i2,i3} \epsilon_{m1,m2,m3}. \quad (111)$$

Simple estimates show that such a state is no longer more economical.

Similarly, one can construct a wave function for infinite diquark matter starting from a set of plane wave states. The ground state would then be a quite peculiar “color crystal”, where the diquark momentum is determined from the balance of kinetic and potential energy, the latter resulting from the color-electric fields. We have not attempted to calculate the energy in this phase, but it seems much more natural to consider a quark-diquark phase.

The quark-diquark (QDQ) phase could occur as an intermediate phase between nuclear matter and the color superconducting phase. Let us focus on a flavor composition corresponding to neutron matter (relevant for dense stars): ud diquarks plus an equal amount of d quarks. In this case, the total color and electric charge are zero. However, if the density is very low, color has to be neutralized over large distances, and confinement prohibits a phase like this. It is amusing to note that even without confinement, there is no low density QDQ phase. One reason is that the nucleon is bound *w.r.t.* a diquark and a quark. Another reason is that at very low density Fermi motion in the QDQ phase is more costly than in the nuclear phase. For example, let us set the threshold for the QDQ phase, $M_{dq} = M_{dq} + M$ equal to the nucleon mass m_N . Then the density of color-compensating d quarks is equal to the density of neutrons in the nuclear phase at the same baryon density. Furthermore, since both have the same degeneracy factor ($g_s=2$ due to spin, the color being fixed by the color of the diquark condensate), both the d quark and the neutron have the same Fermi momentum p_f . The kinetic energy $p_f^2/(2M)$ is then smaller for the neutron because of its larger mass.

Nevertheless, it is not obvious which phase is preferred at densities a few times nuclear matter density. The QDQ phase is very different from both nuclear matter and color superconducting ($N_f = 2$) quark matter, in particular both chiral symmetry and color are broken. This suggests that if such a phase exists, it is probably an isolated minimum, separated by first order transitions on both sides. Let us try to estimate if such a window may exist. We assume that $\langle \bar{q}q \rangle$ is large in this phase, still providing an effective quark mass $\mathcal{O}(400 \text{ MeV})$, and therefore this phase should have no strange component, in contrast to the CSC3. The interactions in nuclear matter crucially combine long range attraction with short range repulsion. A similar description may be approximately valid for diquarks as well. Let us use a simple model, with only repulsive interactions represented by the scattering length² a . The energy per baryon of the diquark Bose gas is

$$\frac{\epsilon_{dq}}{n_B} = \frac{12\pi a n_{dq}}{m} \left(1 + \frac{128}{15\sqrt{\pi}} (a^3 n_{dq})^{1/2} \right), \quad (112)$$

where n_{dq} denotes the diquark density. The first term is just the mean-field interaction of the condensed diquarks, the second term stems from non-condensed bosons, as follows from the classic Lee-Yang paper [56]. In this approximation the unphysical behavior of the ideal Bose gas is overcome, the chemical potential grows with the density, and at some density it becomes favorable to split some diquarks into quarks. We are then led to a mixture of a Bose gas of diquarks and a Fermi gas of quarks (now of the same color), with chemical potentials related by the equilibrium condition $\mu_{dq} = 2\mu$. Such a description leads to a more natural transition to quark matter with Cooper pairs at high density.

²The radius of the nucleon repulsive core is about 0.4 fm, but diquarks (and constituent quarks) are smaller objects. If they are instanton-generated, their core should be of the order of the typical instanton radius $\rho \approx 1/3 \text{ fm}$ [52], which we took as a representative value.

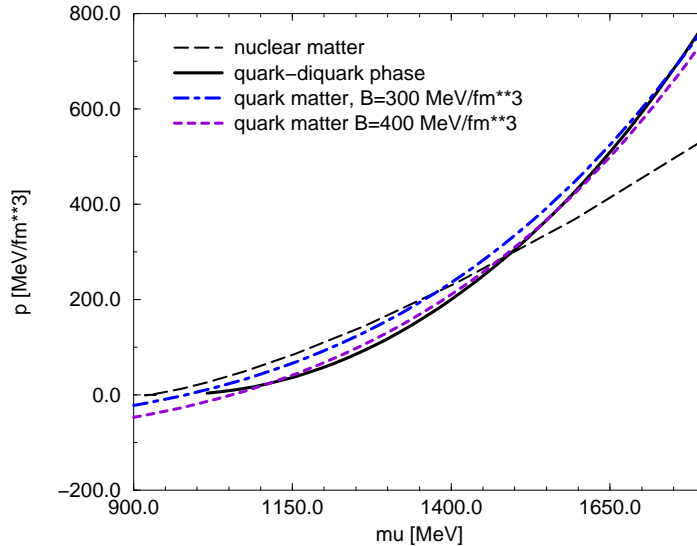


FIG. 14. Pressure versus baryonic chemical potential (3 times μ for quarks as used above) for 3 phases: nuclear matter, the quark-diquark phase made of a Bose gas of interacting diquarks and a Fermi gas of constituent quarks (no bag constant), and a Fermi gas of u, d, s quarks with current masses (for two different bag constants).

So far we have ignored the role of confinement. One possibility is that the transition to the quark-diquark phase leads to deconfinement. If not, one has to include the energy associated with separated color charges. It is well known that the confining potential in vacuum is linear $V(r) = Kr$, with a string tension $K \simeq 1$ GeV/fm. However, for small r this relation only holds for heavy, point-like quarks, not for light ones. Various non-relativistic models of hadronic structure use some effective K , reduced by a significant factor, in order to obtain a good description of hadronic masses. Indeed, it was found on the lattice – by measuring the string tension after smoothing the gauge fields³ – that the effective potential between constituent quarks is very small at small r , but approaches $V(r) = Kr$ at large distances. The motivation for smoothening is due to the extended nature of constituent quarks, as opposed to essentially point-like heavy flavors (c, b). To put it differently: color-strings only form if constituent quarks do not overlap. For such a potential the average energy of colored strings seems to be negligible for the relevant densities considered above.

C. Observable signatures

In this section we would like to discuss potential experimental signatures of the quark-diquark and quark superconducting phases, in particular with regard to heavy-ion experiments and neutron stars. Let us start with the quark-diquark phase. It is easy to estimate the critical temperature for the quark-diquark mixture by applying Einstein's ideal gas expression for Bose condensation

$$T_c = 3.31 n_{dq}^{2/3} / M_{dq} . \quad (113)$$

Assuming $n_{dq} = 3 * n_0$ and $M_{dq} = 0.6$ GeV we find $T_c = 120$ MeV, which is expected to be further reduced by the short range repulsive core. Heavy-ion collisions at SIS/BEVALAC energies (1-2 AGeV), where comparable compression is reached, lead to a heating of the system of up to $T \approx 100$ MeV, and so we conclude that even if this phase exists and our estimates are valid, it can be involved only peripherally. The same is even more true for the color superconducting phase. Because of the high density and low critical temperature of the color superconductor, it is not likely to be produced in heavy-ion collisions.

³For example, the results of [57] can be approximated as $V = K|R - R_0|\theta(R - R_0)$ with the standard string tension $K \simeq 1$ GeV/fm but a rather large $R_0 \simeq 0.7$ fm.

Even if the gap is still larger than expected so that matter in the color superconducting phase would be produced in heavy-ion collisions, its presence will be hard to establish. The two most spectacular manifestations of superconductivity, perfect conductivity and the Meissner effect, are very difficult to detect for a short-lived sample. The transition to the superconducting state has an effect on the equation of state, but the condensation energy $\epsilon \sim \mu \Delta^2 p_F / (2\pi^2)$ is small compared to the energy density of a Fermi gas. In this context, the effect of quark-diquark phase is likely to be larger. Finally, the superconducting phase, in particular color-flavor-locking, may have an effect on the flavor composition. But this effect is not very specific since strangeness enhancement is a general consequence of quark matter formation.

For these reasons, compact stars and stellar explosions are probably a more appropriate place to search for observational consequences of quark superconductivity. For a recent review on the structure of neutron stars we refer the reader to Refs. [58,59]. Owing to theoretical uncertainties in the nuclear equation of state, the central density of neutron stars is not very well known. The main experimental constraint comes from the fact that neutron stars with masses $M_{NS} = 1.45 M_{Sun}$ have definitely been observed. This still allows for central densities as low as $3n_0$ or as high as $10n_0$. Ultimately, a better handle on the central density will come from measurements of neutron star radii.

In neutron star structure calculations quark matter is almost always treated as a simple Fermi gas, confined by a bag constant B . Let us only note here that there are two distinct scenarios: (i) For sufficiently small values of B strange quark matter is absolutely stable, and the entire star is in this phase, while (ii) for large B the outer part of the star consists of nuclear matter, while the interior contains various mixed phases (quark matter sheets, rods or clusters). These funny arrangements owe their existence to the possibility to move charge from the quark phase to the hadronic phase. The shape is then determined by the interplay of the equation of state and long range Coulomb forces. Quark superconductivity will again have an influence on the equation of state, but as before we expect this to be a correction on the order of $\mathcal{O}((\Delta/\mu)^2)$, small compared to the uncertainties in the bag constant.

In neutron stars, a more direct measure of the gap is provided by the cooling history of the star. Without a gap, neutron stars can efficiently cool by β -decay of thermally excited u, d quarks. This process seems to lead to unacceptably large cooling rates [60]. Such a problem emerged already for neutrino emission from nuclear matter. In that case it is solved due to nuclear superfluidity. Since both neutrons and protons are gapped, there are no single-particle states in the vicinity of the Fermi surface. For two-flavor quark matter, a similar problem arises since the quarks of the third color have no or only very small gaps. It is absent in the color-flavor-locked phase, because all quarks acquire a gap. For realistic values of the strange quark mass, the system is likely to be in the two-flavor phase at moderate densities, so that the “cooling-problem” for neutron stars might still persist.

Another feature of the CSC-phases is that Cooper pairs are electrically charged, so one might expect the color superconductor to be electrically superconducting as well. This is not quite true. For both the $N_f = 2$ and color-flavor locked phase, there is a modified charge operator that is not broken, so there is a linear combination of the photon and the diagonal gluons that remains massless. Nevertheless, since the photon inside the superconducting phase is different from the photon outside, magnetic flux will be *partially* expelled. Magnetic fields in pulsars are very large, up to 10^{12} Gauss. Fields on the order of 10^{15} Gauss were recently suggested to drive the so called “magnetars”, and 10^{18} gauss is the absolute upper limit allowed by star stability (virial theorem). However, even such fields are not yet large enough to significantly influence the CSC phase. On the other hand, simple scaling considerations show that in order to have the field completely expelled from the quark matter core would cost energy of order $\mathcal{O}(R^3)$ (where R is the star radius), while transferring the field lines through some channels into the superconductor only costs $\mathcal{O}(R)$. Inside these channels the field should be at the critical value $B_c \sim 10^{19}$ Gauss. They can be either macroscopic (if the superconductor is of the first kind) or microscopic Abrikosov vortices (if it is of the second kind).

X. SUMMARY AND CONCLUSIONS

We have studied the interplay of instantons, superfluidity/-conductivity and chiral symmetry breaking in QCD at finite density. Unlike many schematic models based on short-range interactions abstracted from one gluon exchange, the instanton model has the virtue of providing a realistic phenomenology of the zero-density ground state, including such features as spontaneous chiral symmetry breaking and a correct description of (light) hadron spectroscopy. This gives us some confidence for a semi-quantitative investigation of cold quark matter at moderate densities as might be encountered, *e.g.*, in the core of neutron stars.

We started out by reviewing some properties of the instanton-induced quark-quark interaction at $\mu = 0$: it originates from the same effective interaction that leads to chiral condensation and a light pion in the QCD vacuum, predominantly acting in the scalar-isoscalar, color antitriplet qq channel. We found these correlations to be sufficiently strong to generate a bound-state pole in the corresponding diquark propagator.

In a second step we studied the density dependence of the instanton-induced (‘t Hooft) interaction. It arises through

the modification of the quark zero modes as we introduce a chemical potential. Both the density-dependence of the instanton form factors, governing the effective quark-(anti-)quark interactions, and of the instanton-antiinstanton overlap matrix elements, relevant for a statistical treatment of the instanton liquid, have been assessed. The main difference to earlier calculations (using local approximations or schematic formfactors) manifests itself in quantitatively somewhat larger superconducting gaps ($\sim 150\text{--}200$ MeV).

In the first main part of this article we have performed a systematic study of the finite- μ , $N_c = 3$ -QCD phase structure for 2, 3 and 2+1 flavors within the mean-field approximation:

- (i) For two massless flavors we confirmed the usual transition to a ud superconductor at $\mu_c \simeq 300$ MeV with gaps $\Delta \simeq 200$ MeV. Apart from some quantitative deviations the use of microscopic instanton formfactors entailed the possible existence of a novel intermediate phase, namely chirally broken quark-diquark matter (characterized by simultaneous chiral symmetry breaking and diquark condensation).
- (ii) For three massless flavors we returned to a simplified treatment based on a idealized sharp formfactor (amenable to the more involved calculations with somewhat less accuracy). We found that, like schematic one-gluon exchange interactions, instantons lead to color-flavor locking, despite their very different color-flavor vertex structure. In addition, there emerged an interesting new feature: in contrast to OGE, instantons generate a non-zero (albeit small) chiral condensate in the superfluid phase.
- (iii) The consequences of finite (current) strange quark masses m_s have been investigated. With increasing m_s a sharp phase transition from the color-flavor locked phase to the two-flavor superconductor occurs. At small chemical potential, the critical strange quark mass is smaller than the physical mass. As the chemical potential grows, the critical mass is also expected to grow. We find that the color-flavor locked phase will appear only at $\mu > 450 - 500$ MeV. This implies that chiral symmetry would be restored initially and then broken again at higher density, but with much smaller condensates.

In the second main part of our article a statistical mechanics treatment of the instanton liquid has been employed. This enabled us to incorporate effects that go beyond the standard mean-field approximation, in particular those associated with instanton-antiinstanton molecules. We demonstrated how to handle a complex fermion determinant in this context (using a gluonic interaction that has been averaged over the relative color orientation). Without molecules, the results were shown to be in reasonable agreement with the mean-field analysis in the first part. Including correlations, molecule formation constitutes a $\sim 10\%$ effect in the free energy/critical chemical potential of the $T=0$ -, $N_f = 2$ -transition. However, with rising temperature I - A molecules are expected to play an increasingly important role in the transition between the superconducting and the plasma phases, corresponding to the critical temperature for superconductivity. Furthermore, the statistical mechanics approach allows to assess the μ -dependence of the total instanton density. It turns out that the latter is indeed approximately constant for all μ -values under consideration, which is not really surprising as the gluonic energy within the instanton component carries the dominant fraction of the free energy of the system. This supports the respective assumption made in earlier works as well as in the first part of this article.

Based on our results, we conjectured a qualitative picture of the QCD phase diagram in the T - μ plane. We argued that for realistic values of the strange quark mass, there are both finite- μ and finite- T transitions between the color-flavor locked (CSC3) and two-flavor superconducting (CSC2) states. With increasing density and at small T , chiral symmetry is first restored and then (weakly) broken again. We also elucidated on the possibility of a new quark-diquark phase, in which nucleons are dissolved into a Bose gas of ud -diquarks and a Fermi gas of unpaired quarks, characterized by simultaneously broken color and chiral symmetry. It represents a natural possibility for an intermediate phase between the hadronic and superconducting phase, although numerical estimates for its existence are rather uncertain.

Concerning experimental consequences, we conclude that heavy-ion reactions are unlikely to reach into the rich high-density/low-temperature phase structure discussed here. In this respect neutron stars are much more promising. The pairing gaps should leave their traces in cooling rates and even in the equation of state provided the pairing gaps are large enough. Decomposition of the “external” into “internal” magnetic fields presumably imply complicated configurations inside the stars.

As an outlook, we expect that it should be rather straightforward to generalize our approach to a simultaneous account of finite μ and T . Another major challenge is to go beyond the mean-field approximation in the quark sector in order to address clustering of quarks into nucleons, and, even more difficult, the nucleon-nucleon interaction. The instanton liquid model does provide the correct properties on the one-nucleon level. Turning the instanton liquid into a realistic description of nuclear matter, however, requires a long way to go. These and related issues certainly provide exciting opportunities for future research in the field of finite-density QCD.

ACKNOWLEDGEMENTS

R. R. acknowledges support from the A.-v.-Humboldt foundation as a Feodor-Lynen fellow. T. S. is supported by NSF-PHY-513835. This work is supported in part by US-DOE grants DE-FG02-88ER40388, DE-FG06-90ER40561 and DE-FG02-91-ER40682.

APPENDIX A: FIERZ TRANSFORMATIONS

Let us denote a general four-fermion interaction of the type (9) by $(\bar{\psi}_a \mathcal{O} \psi_b)(\bar{\psi}_c \mathcal{O} \psi_d)$. An effective “mesonic” interaction corresponds to the sum of the direct and exchange ($s+u$) channels. The corresponding kernel is the sum of the original interaction and its Fierz transform:

$$”s + u” = (\bar{\psi}_a \mathcal{O} \psi_b)(\bar{\psi}_c \mathcal{O} \psi_d) + (\bar{\psi}_a \mathcal{O}_1 \psi_d)(\bar{\psi}_c \mathcal{O}_1 \psi_b) . \quad (A1)$$

An effective diquark (t -channel) interaction is obtained by first transposing and then performing the Fierz transformation

$$T = (\bar{\psi}_a \mathcal{O} \psi_b)(\psi_d^T \mathcal{O}^T \bar{\psi}_c^T) = \epsilon(\bar{\psi}_a \mathcal{O} \psi_b)(\psi_d^T C \mathcal{O} C \bar{\psi}_c^T) = \epsilon(\bar{\psi}_a \mathcal{O}_2 C \bar{\psi}_c^T)(\psi_d^T C \mathcal{O}_2 \psi_b) . \quad (A2)$$

We use Euclidean gamma matrices in the standard or chiral representations, $C = -i\gamma_2\gamma_0$, $C^2 = C^\dagger C = \mathbb{1}$. If the isospin and color parts of \mathcal{O} are $\mathbb{1}$, $\epsilon = -1$ if the Dirac part of \mathcal{O} is γ_μ , $\sigma_{\mu\nu}$, and $\epsilon = 1$ when it is $\mathbb{1}_D$, γ_5 , $\gamma_\mu\gamma_5$. For the flavor part, $\tau_2^T = -\tau_2$ and $\tau_{1,3}^T = \tau_{1,3}$.

For the Fierz transformation the following completeness relations are used:

$$\delta_{ii'}\delta_{jj'} = \frac{1}{N_c}\delta_{ij'}\delta_{ji'} + 2t_{ij'}^n t_{ji'}^n \quad (A3)$$

for color,

$$\delta_{AA'}\delta_{BB'} = \frac{1}{2}\delta_{AB'}\delta_{BA'} + \frac{1}{2}\tau_{AB'}^a \tau_{BA'}^a \quad (A4)$$

$$\tau_{AA'}^a \tau_{BB'}^a = \frac{3}{2}\delta_{AB'}\delta_{BA'} - \frac{1}{2}\tau_{AB'}^a \tau_{BA'}^a \quad (A5)$$

for isospin, and, defining $S = \mathbb{1} \otimes \mathbb{1}$, $V = \gamma_\mu \otimes \gamma_\mu$, $P = \gamma_5 \otimes \gamma_5$, $A = \gamma_5 \gamma_\mu \otimes \gamma_\mu$, $T = \sigma_{\mu\nu} \otimes \sigma_{\mu\nu}$, with $\sigma_{\mu\nu} = 1/2[\gamma_\mu, \gamma_\nu]$,

$$\begin{pmatrix} S \\ V \\ T \\ A \\ P \end{pmatrix}' = \begin{pmatrix} 1/4 & 1/4 & -1/8 & -1/4 & 1/4 \\ 1 & -1/2 & 0 & -1/2 & -1 \\ -3 & 0 & -1/2 & 0 & -3 \\ -1 & -1/2 & 0 & -1/2 & 1 \\ 1/4 & -1/4 & -1/8 & 1/4 & 1/4 \end{pmatrix} \begin{pmatrix} S \\ V \\ T \\ A \\ P \end{pmatrix} \quad (A6)$$

for the Dirac structures. Due to the tensor product structure of the matrices \mathcal{O} , one has to Fierz transform separately the Dirac, color and isospin parts by using the above relations and multiply them accounting for the fact that fermion fields anticommute. The latter generates an additional (-1) in the u -channel, and for the t -channel it excludes any symmetric parts of the \mathcal{O}' matrices. The final results are given in the main text, Eqs. (10) and (11).

APPENDIX B: INSTANTON FORM FACTORS AT FINITE μ

The two structures in the form factor are

$$B = 4\rho i \int_0^\infty dR R^3 \int_0^\pi d\eta \sin^2 \eta \frac{1}{R\sqrt{R^2 + \rho^2}} \left[\left(1 - 2\frac{t^2}{R^2 + \rho^2} - \mu t \right) \frac{\sin(\mu r)}{r} - \left(2\frac{t}{R^2 + \rho^2} + \mu \right) \cos(\mu r) \right] \frac{\sin(kr)}{kr} e^{-i\omega t} \quad (B1)$$

$$A = -4\rho \int_0^\infty dR R^3 \int_0^\pi d\eta \sin^2 \eta \frac{1}{R\sqrt{R^2 + \rho^2}} \left[-\left(\mu + \frac{t}{r^2} + \frac{2t}{R^2 + \rho^2} \right) \sin(\mu r) + \left(\frac{\mu t}{r} - \frac{2r}{R^2 + \rho^2} \right) \cos(\mu r) \right] \left(\frac{\cos(kr)}{kr} - \frac{\sin(kr)}{k^2 r^2} \right) e^{-i\omega t} . \quad (B2)$$

Let us separate the real and imaginary parts of A and B : $A = A_c + iA_s$, $B = B_s + iB_c$, the subscript referring to $\cos(\omega t)$ or $\sin(\omega t)$. We also introduce $k^\pm = k \pm \mu$. Then

$$A_c = \frac{2\rho}{k} \int_0^\infty dR \int_0^\pi d\eta \frac{R \sin \eta \cos(\omega R \cos \eta)}{\sqrt{R^2 + \rho^2}} \left[\left(\frac{2R \sin \eta}{R^2 + \rho^2} + \frac{\mu}{kR \sin \eta} \right) \cos(k^+ R \sin \eta) + \left(\mu - \frac{2}{k(R^2 + \rho^2)} \right) \sin(k^+ R \sin \eta) \right] + (\mu \rightarrow -\mu) \quad (B3)$$

$$A_s = \frac{-i2\rho}{k} \int_0^\infty dR \int_0^\pi d\eta \frac{R \cos \eta \sin(\omega R \cos \eta)}{\sqrt{R^2 + \rho^2}} \left[\left(\frac{1}{kR^2 \sin^2 \eta} + \frac{2}{k(R^2 + \rho^2)} - \mu \right) \cos(k^+ R \sin \eta) + \left(\frac{k^+}{kR \sin \eta} + \frac{2R \sin \eta}{R^2 + \rho^2} \right) \sin(k^+ R \sin \eta) \right] - (\mu \rightarrow -\mu) \quad (B4)$$

$$B_c = \frac{-i2\rho}{k} \int_0^\infty dR \int_0^\pi d\eta \frac{\cos(\omega R \cos \eta)}{\sqrt{R^2 + \rho^2}} \left[\left(1 - \frac{2R^2 \cos^2 \eta}{R^2 + \rho^2} \right) \cos(k^+ R \sin \eta) + \mu R \sin \eta \sin(k^+ R \sin \eta) \right] - (\mu \rightarrow -\mu) \quad (B5)$$

$$B_s = \frac{2\rho}{k} \int_0^\infty dR \int_0^\pi d\eta \frac{R \cos \eta \sin(\omega R \cos \eta)}{\sqrt{R^2 + \rho^2}} \left[\mu \cos(k^+ R \sin \eta) - \frac{2R \sin \eta}{R^2 + \rho^2} \sin(k^+ R \sin \eta) \right] + (\mu \rightarrow -\mu) . \quad (B6)$$

Using the following basic integrals,

$$\int_0^\pi d\eta \cos(\alpha \cos \eta) \cos(\beta \sin \eta) = \pi J_0(\sqrt{\alpha^2 + \beta^2}) \quad (B7)$$

and, denoting $\omega^\pm = \sqrt{\omega^2 + (k^\pm)^2}$,

$$\int_0^\infty dR \frac{1}{\sqrt{R^2 + \rho^2}} J_0(R\omega^\pm) = I_0\left(\frac{\rho\omega^\pm}{2}\right) K_0\left(\frac{\rho\omega^\pm}{2}\right) \equiv I_0^\pm K_0^\pm, \quad (B8)$$

one can rewrite the above expressions as derivatives of $I_0^\pm K_0^\pm$ according to

$$A_c = \frac{2\pi\rho}{k} \left[\frac{2}{\rho} \frac{d}{d\rho} \left(\frac{d^2}{dk^2} - \frac{1}{k} \frac{d}{dk} \right) + \mu \left(\frac{1}{k} - \frac{d}{dk} \right) \right] I_0^+ K_0^+ + (\mu \rightarrow -\mu), \quad (B9)$$

$$A_s = \frac{i2\pi\rho}{k} \left[\frac{d}{d\omega} \left(\frac{2}{\rho} \frac{d}{d\rho} \left(\frac{d}{dk} - \frac{1}{k} \right) - \mu \right) I_0^+ K_0^+ + \int_0^\mu d\mu' \frac{k^+}{k} \frac{d}{d\omega} I_0^+ K_0^+ \right] - (\mu \rightarrow -\mu) . \quad (B10)$$

Using $\frac{d}{d\omega} = \frac{\omega}{\omega^+} \frac{d}{d\omega^+}$, $\frac{d}{d\mu} = \frac{k^+}{\omega^+} \frac{d}{d\omega^+}$, the integral over μ' is just $\frac{\omega}{k} I_0^+ K_0^+$. Furthermore,

$$B_c = \frac{i2\pi\rho}{k} \left(1 - \frac{2}{\rho} \frac{d}{d\rho} \frac{d^2}{d\omega^2} - \mu \frac{d}{dk} \right) I_0^+ K_0^+ - (\mu \rightarrow -\mu), \quad (B11)$$

$$B_s = \frac{-2\pi\rho}{k} \left(\mu - \frac{2}{\rho} \frac{d}{d\rho} \frac{d}{dk} \right) \frac{d}{d\omega} I_0^+ K_0^+ + (\mu \rightarrow -\mu). \quad (B12)$$

Denoting $\frac{d}{dz} I_0^+ K_0^+ = I_1^+ K_1^+ - I_0^+ K_1^+ \equiv \Delta^+$, we get

$$A_c = \frac{2\pi\rho}{k} \left[\left(\frac{\mu}{k} + \frac{2(k^+)^2}{(\omega^+)^2} \right) I_1^+ K_1^+ + \frac{\rho k^+}{2\omega^+} (2k + \mu) \Delta^+ \right] + (\mu \rightarrow -\mu), \quad (B13)$$

$$A_s = \frac{i2\pi\rho}{k} \left[\left(\frac{\omega}{k} + \frac{2\omega k^+}{(\omega^+)^2} \right) I_1^+ K_1^+ + \frac{\rho\omega}{2\omega^+} (2k + \mu) \Delta^+ \right] - (\mu \rightarrow -\mu), \quad (B14)$$

$$B_c = \frac{i2\pi\rho}{k} \left[\frac{\omega^2 - (k^+)^2}{(\omega^+)^2} I_1^+ K_1^+ + \frac{\rho}{2\omega^+} (2\omega^2 + \mu k^+) \Delta^+ \right] - (\mu \rightarrow -\mu), \quad (B15)$$

$$B_s = \frac{2\pi\rho}{k} \left[\frac{2\omega k^+}{(\omega^+)^2} I_1^+ K_1^+ + \frac{\rho\omega}{2\omega^+} (2k + \mu) \Delta^+ \right] + (\mu \rightarrow -\mu). \quad (B16)$$

These Fourier transforms of the fermion zero modes at finite μ agree with the results obtained in [13].

APPENDIX C: GRAND CANONICAL POTENTIAL IN THE CORNWALL-JACKIW-TOMBOULIS (CJT) FORMALISM

To derive the grand canonical potential in MFA we start from a generating functional with bilocal meson and diquark sources,

$$\exp(W[J, \bar{J}, K, \bar{K}]) = \int \mathcal{D}\psi \mathcal{D}\bar{\psi} \exp \left\{ (S_0 + U + \int \bar{\psi} J \psi + \int \psi^T \bar{J} \bar{\psi}^T + \int \bar{\psi} \bar{K} \bar{\psi}^T + \int \psi^T K \psi) \right\}, \quad (C1)$$

where S_0 is the free fermion action and $U = \int (\mathcal{L}_{mes} + \mathcal{L}_{diq})$ with $\mathcal{L}_{mes}, \mathcal{L}_{diq}$ given in Eqs. (10,11). Using a matrix representation, we write the free part of the action in momentum space as

$$\begin{aligned} S_0 &= \int \frac{d^4 p}{(2\pi)^4} \left[\bar{\psi}(p)(J(p) + \frac{1}{2}G_0^{-1}(p))\psi(p) + \psi^T(-p)(\bar{J}(p) \right. \\ &\quad \left. + \frac{1}{2}G_0^{-1T}(-p))\bar{\psi}^T(-p) + \bar{\psi}(p)\bar{K}(p)\bar{\psi}^T(-p) + \psi^T(-p)K\psi(p) \right] \\ &= \int \frac{d^4 p}{(2\pi)^4} \begin{pmatrix} \bar{\psi}(p), & \psi^T(-p) \end{pmatrix} \begin{pmatrix} \bar{K}(p) & J(p) + \frac{1}{2}G_0^{-1}(p) \\ \bar{J}(p) - \frac{1}{2}G_0^{-1T}(-p) & K(p) \end{pmatrix} \begin{pmatrix} \bar{\psi}^T(-p) \\ \psi(p) \end{pmatrix}, \end{aligned} \quad (C2)$$

where the sources J, \bar{J}, K, \bar{K} have the following properties:

$$\begin{aligned} -\bar{J}^T(-p) &= J(p) \\ -\bar{K}^T(-p) &= \bar{K}(p) \\ -K^T(-p) &= K(p). \end{aligned} \quad (C3)$$

The path integral over the fermion fields is

$$\begin{aligned} e^{W_0} &= \int \mathcal{D}\psi \mathcal{D}\bar{\psi} e^S = \det^{\frac{1}{2}} \begin{pmatrix} \bar{K} & J + \frac{1}{2}G_0^{-1} \\ \bar{J} - \frac{1}{2}G_0^{-1T} & K \end{pmatrix} \equiv \det \mathcal{M} \\ W_0 &= \frac{1}{2} \text{tr} \ln \mathcal{M}, \end{aligned} \quad (C4)$$

where the trace includes the momentum integration, and the products between the fields (sources) include convolutions in momentum as well as all other indices. Using the identities

$$\begin{aligned} \begin{pmatrix} \bar{A} & B \\ \bar{B} & A \end{pmatrix} &= \begin{pmatrix} 0 & B \\ \bar{B} & 0 \end{pmatrix} \begin{pmatrix} \mathbb{1} & \bar{B}^{-1}A \\ B^{-1}\bar{A} & \mathbb{1} \end{pmatrix}, \\ \ln \det \begin{pmatrix} \bar{A} & B \\ \bar{B} & A \end{pmatrix} &= \ln \det(-B\bar{B}) + \text{tr} \ln(1 + \begin{pmatrix} 0 & \bar{B}^{-1}A \\ B^{-1}\bar{A} & 0 \end{pmatrix}) \\ &= \ln \det(-B\bar{B}) + \text{tr} \sum_{n=1}^{\infty} \frac{(-1)^{n-1}}{n} \begin{pmatrix} 0 & \bar{B}^{-1}A \\ B^{-1}\bar{A} & 0 \end{pmatrix}^n \\ &= \ln \det(-B\bar{B}) + \text{tr} \sum_{n=1}^{\infty} -\frac{1}{2n} (\bar{B}^{-1}A B^{-1}\bar{A} + B^{-1}\bar{A} \bar{B}^{-1}A) \\ &= \ln \det(-B\bar{B}) + \text{tr} \ln(1 - \bar{B}^{-1}A B^{-1}\bar{A}) \\ &= \text{tr} \ln(-B\bar{B} + BAB^{-1}\bar{A}), \end{aligned} \quad (C5)$$

we obtain

$$W_0 = \frac{1}{2} \text{tr} \ln [-(J + \frac{1}{2}G_0^{-1})(\bar{J} - \frac{1}{2}G_0^{-1T}) + (J + \frac{1}{2}G_0^{-1})K(J + \frac{1}{2}G_0^{-1})^{-1}\bar{K}]. \quad (C6)$$

Next, one introduces the classical two-point fields $\bar{F} = \frac{\delta W}{\delta K}$, $F = \frac{\delta W}{\delta \bar{K}}$, $G = \frac{\delta W}{\delta J}$, $\bar{G} = \frac{\delta W}{\delta \bar{J}}$ and performs a Legendre transformation

$$\Gamma[G, \bar{G}, F, \bar{F}] = W[J, \bar{J}, K, \bar{K}] - \text{tr}(GJ + \bar{G}\bar{J} + KF + \bar{K}\bar{F}) \quad (\text{C7})$$

with J, \bar{J}, K, \bar{K} expressed as functionals of G, \bar{G}, F, \bar{F} . From the non-interacting part W_0 we have

$$\begin{aligned} G &= \frac{1}{2}(J + \frac{1}{2}G_0^{-1} - \bar{K}(\bar{J} - \frac{1}{2}G_0^{-1T})^{-1}K)^{-1} \\ \bar{G} &= \frac{1}{2}(\bar{J} - \frac{1}{2}G_0^{-1T} - K(J + \frac{1}{2}G_0^{-1})^{-1}\bar{K})^{-1} \\ F &= -(J + \frac{1}{2}G_0^{-1})^{-1}\bar{K}\bar{G} \\ \bar{F} &= -(\bar{J} - \frac{1}{2}G_0^{-1T})^{-1}K)^{-1}KG, \end{aligned} \quad (\text{C8})$$

and

$$\Gamma_0 = -\frac{1}{2}\text{tr} \ln(-\bar{G}G + \bar{G}F\bar{G}^{-1}\bar{F}) + \frac{1}{2}\text{tr}(G_0^{-1}G - G_0^{-1T}\bar{G} - 2). \quad (\text{C9})$$

Following the CJT approach [39] for the four-fermion interaction, one can show that

$$\Gamma = \Gamma_0 + \frac{1}{4!}\hbar^2 \left(\text{tr}(G \frac{\delta^2}{\delta\psi\delta\bar{\psi}}) S_{\text{int}} \text{tr}(\frac{\overleftarrow{\delta^2}}{\delta\psi\delta\bar{\psi}} \bar{G}) + \text{tr}(F \frac{\delta^2}{\delta\bar{\psi}^T\delta\psi}) S_{\text{int}} \text{tr}(\frac{\overleftarrow{\delta^2}}{\delta\psi\delta\bar{\psi}^T} \bar{F}) \right) + \Gamma_4, \quad (\text{C10})$$

where S_{int} is the original four-fermion interaction and we have explicitly indicated the dependence on \hbar . Now it becomes clear that, in order to perform the functional derivatives, it is convenient to Fierz-rearrange S_{int} into the 3 channels s, t and u as outlined above. The sum of the four derivatives in Eq. (C10) naturally suggests the use of U in Eq. (C1) with two-by-two derivatives *w.r.t.* the fermion fields that are contracted with the same matrix \mathcal{O}^i .

The Hartree-Fock scheme is equivalent to (i) neglecting Γ_4 , which is the sum of all four-particle irreducible diagrams and is of order $O(\hbar^4)$, and (ii) considering only translationally invariant solutions (*e.g.*, $G(p, p') = G(p)\delta^4(p - p')$, and the same for F, \bar{F}). The mesonic and the diquark terms in the above lowest-order interaction term have the form $V_4(\mathbf{M}_i)(\bar{\mathbf{M}}_i), V_4(\mathbf{D}_i)(\bar{\mathbf{D}}_i)$, where

$$\begin{aligned} \mathbf{M}_i &= \int \frac{d^4p}{(2\pi)^4} \text{tr}(G g_i^{\text{mes}} \mathcal{F}^\dagger \mathcal{O}^i \mathcal{F}) \\ \mathbf{D}_i &= \int \frac{d^4p}{(2\pi)^4} \text{tr}(F^\dagger g_i^{\text{diq}} \mathcal{F}^T \mathcal{O}^i C \mathcal{F}^*) , \end{aligned} \quad (\text{C11})$$

i.e., they are products of mesonic and diquark condensates. A priori one might consider condensation in any channel, and then study if it is energetically favored. It is reasonable to start with the channels that are most attractive (*e.g.*, those which generate bound states in vacuum). As we have seen in sects. II and III, these are the scalar color singlet mesonic channel and the diquark color- $\bar{\mathbf{3}}$ one. For the $N_f = 2$ case there is only one pattern of diquark condensation, which necessarily breaks the color symmetry down from $SU(3)_C \rightarrow SU(2)_C$. The diquark condensate is proportional to a unit vector in $SU(3)_C$. Moreover, because the flavor part of the vertex is antisymmetric (due to τ_2), the Pauli principle requires that the above unit vector belongs to the antisymmetric part of $SU(3)_C$. Without loss of generality we can choose this vector to be the Gell-Mann matrix λ_2 (recall that all Gell-Mann matrices in this paper are normalized to 3, *i.e.*, $\text{tr}\lambda_i^2 = 3$). We can identify the unbroken $SU(2)_C$ with the upper 2×2 corner of the $SU(3)_C$ group. If both qq and $\bar{q}q$ condensates are present, the latter should consist of two parts – one that involves the two colors from the unbroken $SU(2)_C$ and the second one which involves quarks and antiquarks from the third color. One should note that there are two terms in \mathcal{L}_{mes} contributing to the $\bar{q}q$ condensates: the isoscalar color singlet one and the isoscalar $SU(3)_C$ octet one proportional to λ_8 . Both have projections onto the $SU(2)_C$ singlet as well as onto the subgroup represented by third color of (unpaired) quarks. Owing to the two different chiral condensates, it is convenient to split the propagators G, \bar{G} into a $SU(2)_C$ part G_1, \bar{G}_1 and a part involving the third color only, G_2, \bar{G}_2 . The F and \bar{F} propagators are proportional to the diquark condensate and hence to λ_2 . Putting everything together, Eq. (C10) becomes

$$\begin{aligned} \Gamma &= -\frac{1}{2}\text{tr} \ln(-\bar{G}_1 G_1 + \bar{G}_1 F \bar{G}_1^{-1} \bar{F}) + \frac{1}{2}\text{tr}(G_0^{-1} G_1 - G_0^{-1T} \bar{G}_1 - 2) \\ &\quad -\frac{1}{2}\text{tr} \ln(-\bar{G}_2 G) + \frac{1}{2}\text{tr}(G_0^{-1} G_2 - G_0^{-1T} \bar{G}_2 - 2) \end{aligned}$$

$$\begin{aligned}
& +g\frac{1}{8N_c^2}|\text{tr}(G_1 + G_2)\alpha|^2 + g\frac{N_c - 2}{16N_c^2(N_c^2 - 1)}|\text{tr}\lambda_8(G_1 + G_2)\alpha|^2 \\
& +g\frac{1}{8N_c^2(N_c - 1)}\text{tr}(FC\gamma_5\lambda_2\tau_2\beta)\text{tr}(\beta^*C\gamma_5\lambda_2\tau_2\bar{F}),
\end{aligned} \tag{C12}$$

where α and β are the formfactors defined in Eqs. (37),(39).

Since G, \bar{G}, F, \bar{F} are classical fields, Γ should vanish under the respective variations.

APPENDIX D: GAP-INDUCED DAMPING OF SINGLE-QUARK PROPAGATORS

In the superconducting phases, single-quark propagation in the vicinity of the Fermi surface is damped in the temporal direction due to the presence of the finite energy gap. This effect has to be included in the evaluation of the I - A overlap matrix elements, Eq. (40), at finite density (this is particularly crucial for the activity z_d of Eq. (91), which otherwise would diverge). Rewriting the overlap matrix elements as

$$T_{IA} = - \int d^4x \left[\phi_I^\dagger(x - z_I; -\mu)(i \not{\partial} - i\mu\gamma_4) \right] (i \not{\partial} - i\mu\gamma_4)^{-1} \left[(i \not{\partial} - i\mu\gamma_4)\Psi_{0,A}(x - z_A; \mu) \right], \tag{D1}$$

they are readily interpreted as a quark hopping amplitude, represented by two amputated (anti-) instanton vertices and an intermediate (free) quark propagator $(i \not{\partial} - i\mu\gamma_4)^{-1}$. In the following we will evaluate an approximate damping factor for this propagator. Starting from the expression of the (massless) momentum space propagator at finite μ in the superconducting phase (ignoring the Dirac structure)

$$\begin{aligned}
G(p, \mu, \Delta) &= \frac{p_0 + \xi}{p_0^2 - \xi^2 - \Delta^2 + i\eta} \\
&= \frac{u_p^2}{p_0 - \epsilon(p) + i\eta} + \frac{v_p^2}{p_0 + \epsilon(p) - i\eta}
\end{aligned} \tag{D2}$$

($\xi = \omega_p - \mu, \epsilon(p)^2 = \xi^2 + \Delta^2, u_p^2 = \frac{1}{2}[1 + \xi/\epsilon(p)], v_p^2 = \frac{1}{2}[1 - \xi/\epsilon(p)]$), we compute its Fourier transform as

$$\begin{aligned}
G(z; \mu, \Delta) &= \int \frac{d^4p}{(2\pi)^4} e^{-ipz} G(p, \mu, \Delta) \\
&= \frac{1}{2\pi^2 r} \int_{p_F}^{\infty} p dp \sin(pr) e^{-\epsilon(p)z_4} u_p^2.
\end{aligned} \tag{D3}$$

For $\Delta \rightarrow 0$ one recovers the result [38]

$$G(z; \mu) = \frac{1}{2\pi^2 z^4} \left[(2z_4 + \mu z^2) \cos(\mu r) + (z_4^2 - r^2 + \mu z_4 z^2) \frac{\sin(\mu r)}{r} \right]. \tag{D4}$$

An approximate correction to $T_{IA}(z; \mu)$ is thus obtained by supplying it with the ratio

$$R(z_4; \mu, \Delta) \equiv \frac{G(z_4; \mu, \Delta)}{G(z_4; \mu)}, \tag{D5}$$

where we have restricted the *l.h.s* of Eq. (D5) to $r=0$ to avoid artificial singularities caused by oscillations in $G(z_4, r; \mu)$. However, since (for $N_f = 2$) only two out of three quarks at the Fermi surface can participate in the diquark condensate, the correction (D5) enters on average with a smaller power, *i.e.*,

$$T_{IA}(z; \mu, \Delta) \simeq R(z_4; \mu, \Delta)^{2/3} T_{IA}(z; \mu). \tag{D6}$$

The net effect of $R(z_4; \mu, \Delta)$ is a damping of the zero mode propagation, which, in fact, is much less pronounced than the naive expectation, $\propto e^{-\Delta z_4}$, would suggest. On the other hand, Ω_{inst} *disfavors* finite values for Δ .

- [1] M. Alford, K. Rajagopal and F. Wilczek, Phys. Lett. B422 (1998), 247.
- [2] R. Rapp, T. Schäfer, E. V. Shuryak and M. Velkovsky, Phys. Rev. Lett. 81 (1998), 53.
- [3] M. Alford, K. Rajagopal and F. Wilczek, Nucl. Phys. B537 (1999), 443.
- [4] T. Schäfer and F. Wilczek, Phys. Rev. Lett. 82 (1999), 3956.
- [5] J. Berges and K. Rajagopal, Nucl. Phys. B538 (1999), 215.
- [6] M. A. Halasz, A. D. Jackson, R. E. Shrock, M. A. Stephanov and J. J. M. Verbaarschot, Phys. Rev. D58 (1998), 096007.
- [7] M. A. Stephanov, K. Rajagopal and E. V. Shuryak, Phys. Rev. Lett. 81 (1998), 4816.
- [8] S. C. Frautschi, *Asymptotic freedom and color superconductivity in dense quark matter*, Proc. of the Workshop on Hadronic Matter at Extreme Energy Density, N. Cabibbo (Editor), Erice, Italy (1978).
- [9] F. Barrois, Nucl. Phys. B129 (1977), 390.
- [10] D. Bailin and A. Love, Phys. Rep. 107 (1984), 325.
- [11] D.T. Son, Phys. Rev. D59 (1999), 094019.
- [12] G.W. Carter and D. Diakonov, Proc. of the International Workshop on 'QCD at Finite Density, Bielefeld, April 27-30 1998, Nucl. Phys. A642 (1998), 78.
- [13] G.W. Carter, D. Diakonov, Phys. Rev. D60 (1999), 016004.
- [14] M. Velkovsky, Proc. of the International Workshop on 'QCD at Finite Density, Bielefeld, April 27-30 1998, Nucl. Phys. A642 (1998), 58.
- [15] T. Schäfer and E.V. Shuryak, Rev. Mod. Phys. 70 (1998), 323.
- [16] M.C. Chu and S. Schramm, Phys. Rev. D51 (1995), 4580.
- [17] B. Alles, M. D'Elia and A. Di Giacomo, Nucl. Phys. B494 (1997), 281.
- [18] T.L. Ivanenko and J.W. Negele, Nucl. Phys. Proc. Suppl. 63 (1998), 504.
- [19] S. Thurner, M.C. Feurstein and H. Markum, Phys. Rev. D56 (1997), 4039.
- [20] T. Schäfer and E.V. Shuryak, Phys. Rev. D53 (1996), 6522.
- [21] P. de Forcrand, M. Garcia Perez, J.E. Hetrick, E. Laermann, J.F. Lagae, I. O. Stamatescu, Nucl. Phys. Proc. Suppl. 73 (1999), 578.
- [22] E.V. Shuryak and M. Velkovsky, Phys. Lett. B437 (1997), 398.
- [23] D.I. Diakonov, V.Yu. Petrov, *Spontaneous breaking of chiral symmetry in the instanton vacuum*, preprint LNPI-1153 (1986), published in: Hadron matter under extreme conditions, Kiev (1986) p. 192.
- [24] W. Pauli, Nuovo Cimento 6 (1957), 205; F. Gürsey, *ibid.* 7 (1958), 411.
- [25] D. Diakonov, H. Forkel and M. Lutz, Phys. Lett. B373 (1996), 147.
- [26] E.-M. Ilgenfritz and E.V. Shuryak, Phys. Lett. B325 (1994), 263.
- [27] M. Velkovsky and E.V. Shuryak, Phys. Rev. D56 (1997), 2766.
- [28] T. Schäfer, E.V. Shuryak and J.J.M. Verbaarschot, Phys. Rev. D51 (1995), 1267.
- [29] R.G. Bettman and L.V. Laperashvili, Yad. Fiz. (Sov. J. of Nucl. Phys.) 41 (1985), 463.
- [30] T. Schäfer, E.V. Shuryak and J.J.M. Verbaarschot, Nucl. Phys. B412 (1994), 143.
- [31] M. Hess, F. Karsch, E. Laermann and I. Wetzorke, Phys. Rev. D58 (1998), 111502.
- [32] M. Anselmino et al., Rev. Mod. Phys. 65 (1993), 1199.
- [33] C.A. De Carvalho, Nucl. Phys. B183 (1980), 182.
- [34] A.A. Abrikosov Jr., Sov. J. of Nucl. Phys. 37 (1983), 459.
- [35] A.A. Abrikosov, L.P. Gorkov, and I.E. Dzyaloshinski, *Methods of Quantum Field Theory in Statistical Physics*, Prentice Hall, Englewood Cliffs, New Jersey 1963.
- [36] E.V. Shuryak and J.J.M. Verbaarschot, Nucl. Phys. B364 (1991), 255.
- [37] R. Rapp, Proc. of the International Workshop on 'QCD at Finite Density', Bielefeld, April 27-30 1998, Nucl. Phys. A642 (1998), 71.
- [38] T. Schäfer, Phys. Rev. D57 (1998), 3950.
- [39] J.M. Cornwall, R. Jackiw and E. Tombolis, Phys. Rev. D10 (1974), 2428.
- [40] E.V. Shuryak and M. Velkovsky, Phys. Rev. D50 (1994), 3323.
- [41] M.A. Shifman and A.I. Vainshtein and V.I. Zakharov, Nucl. Phys. B163 (1980), 46.
- [42] M.A. Nowak and J.J.M. Verbaarschot and I. Zahed, Nucl. Phys. B324 (1989), 1.
- [43] D.I. Diakonov, Proc. of the International Enrico Fermi School in Physics, Varenna, Italy (1995), and hep-ph/9602375.
- [44] R. Shankar, Rev. Mod. Phys. 66 (1995), 129.
- [45] N. Evans, S. D. H. Hsu, M. Schwetz, Nucl. Phys. B551 (1999), 275.
- [46] T. Schäfer and F. Wilczek, Phys. Lett. B450 (1999), 325.
- [47] R. Pisarski and D. Rischke, Phys. Rev. Lett. 83 (1999), 37.
- [48] T. Schäfer and F. Wilczek, hep-ph/9903503.
- [49] M. Alford, J. Berges, and K. Rajagopal, hep-ph/9903502.
- [50] E.-M. Ilgenfritz and S. Thurner, hep-lat/9810010.
- [51] E.-M. Ilgenfritz and E.V. Shuryak, Nucl. Phys. B319 (1989), 511.
- [52] E. V. Shuryak, Phys. Lett. 79B (1978), 135; Nucl. Phys. B203 (1982), 140.
- [53] M. Buballa, Nucl. Phys. A611 (1996), 393.

- [54] M.A. Nowak, Acta Phys. Pol. B22 (1991), 697.
- [55] A.B. Migdal et al., Phys. Rep. 192 (1990), 179;
D.B. Kaplan and A.E. Nelson, Phys. Lett. B175 (1986), 57;
G.E. Brown and H.A. Bethe, Astrophys. J. 423 (1994), 659.
- [56] T.D. Lee and C.N. Yang, Phys. Rev. 105 (1957), 1119.
- [57] M. Feurstein, E.-M. Ilgenfritz, H. Müller-Preussker and S. Thurner, Nucl. Phys. B511 (1998), 421.
- [58] H. Heiselberg and M. Hjorth-Jensen, to be published in Phys. Rep., and nucl-th/9902033.
- [59] H. Heiselberg, C. Pethick, and E. Staubo, Nucl. Phys. A566 (1994), 577c.
- [60] N. Iwamoto, Ann. Phys. 141 (1982), 1.